

**Promotion of protoporphyrin IX (PpIX) fluorescence by MEK inhibition in animal  
models of cancer**

By Ema Yoshioka

A thesis submitted to the  
School of Graduate Studies  
in partial fulfillment of the  
requirements for the degree of  
Masters in Science.

Division of Biomedical Sciences  
Faculty of Medicine  
Memorial University  
**October, 2016**

## Abstract

**Background:** Protoporphyrin IX (PpIX) is an endogenous fluorescence that is accumulated in cancer cells treated with the heme precursor 5-aminolevulinic acid (5-ALA). The cancer-specific fluorescence of PpIX is used to distinguish tumor from normal tissue, which has proven clinically useful during fluorescence-image guided surgery. This study sought to investigate whether modulation of oncogenic Ras/MEK pathway mediates PpIX accumulation *in vitro* and *in vivo*.

**Methods:** For *in vitro* studies, human breast, lung and prostate cancer cells were treated with or without the MEK inhibitor (U0126) for 20 hours, followed with 5-ALA for 5 hours. The cells were lysed, and the PpIX fluorescence accumulated in the cells was measured with a microplate fluorescence reader ( $\lambda_{ex}$  405 nm;  $\lambda_{em}$  635 nm). For *in vivo* studies, the 4T1 mouse breast cancer cells were injected into the right hind flank of 8 week-old Balb/c female mice. U0126 (50  $\mu$ M/Kg) was injected intratumorally to 4T1 breast tumors for 5/8 h followed by 5-ALA injection. Mice bearing 4T1 breast tumors were also injected intraperitoneally with U0126 for 5 or 8. Furthermore, similar experiments were conducted using a HRAS transgenic mice, which develop spontaneous mammary tumors within 3 months old. **Results:** *In vitro*, MEK inhibition increases PpIX fluorescence in human cancer cell lines, but not in normal cell lines. The promotion of PpIX fluorescence by MEK inhibition was most commonly observed among human breast cancer cells. *In vivo*, PpIX accumulation was observed significantly more in the tumors from mice treated with U0126 and 5-ALA (2-3 fold) than those from mice with vehicle control (DMSO/saline) and 5-ALA.

**Conclusions:** *In vitro* and *in vivo* treatment of the MEK inhibitor significantly increases the accumulation of PpIX fluorescence in cancer cells which may contribute to improved efficacy of FGS in clinical settings.

## **Acknowledgement**

I would like to thank my supervisor Dr Kensuke Hirasawa who gave me the opportunity to do this project and for the continuous support of my master study and related research, for his patience, motivation, and immense knowledge.

I would like to thank my co-supervisor Dr Ann Dorward. Whenever I ran into a trouble spot or had a question about my research or writing she always support me. I would not have been able to complete my master's project without her guidance.

I would also like to thank my thesis committee Dr Sheila Drover for the encouragement and advice which incented me to widen my research from various perspectives.

I thank my fellow lab mates (leena, Yumiko, Maria, Vipin, Seyd) for their support, for the days we were working together, and for all the fun we have had. Special thanks to Lenna, without her input and support this project wasn't possible.

My friends and family back home and St John's, for their support and for making me feel better in bad days. Special thanks to my best friend Monio for all the countless support and positive energy.

Last, but of course, not least, I would like to thank my family: my mother, and father, brother, and Dorna. It is because of them and their never-ending support, love, encouragement, and belief in that I can do whatever I put my mind to, which has made this thesis possible.

## Table of Contents

<b>Abstract</b> .....	I
<b>Acknowledgement</b> .....	II
<b>List of Tables</b> .....	VI
<b>List of Figures</b> .....	VII
<b>List of Abbreviations</b> .....	VIII
<b>Chapter 1: Introduction</b> .....	1
<b>1.1 Therapeutic strategies for cancer treatment</b> .....	1
<b>1.1.1 Fluorescence-Guided Surgery</b> .....	4
<b>1.1.2 Properties of Fluorophores</b> .....	6
<b>1.1.3 Basic features of Fluorescence-guided surgical practice</b> .....	9
<b>1.1.4 Fluorescence contrast agents</b> .....	9
<b>1.1.4.1 Exogenous fluorescence</b> .....	10
<b>1.1.4.1.1 Non-specific fluorescence contrast agents:</b> .....	10
<b>1.1.4.1.2 Tumour-specific fluorescence contrast agents:</b> .....	10
<b>1.1.4.2 Endogenous fluorescence</b> .....	10
<b>1.2 PpIX is an intermediate of the heme biosynthesis pathway</b> .....	16
<b>1.2.1 5-Aminolevulinic Acid (5-ALA) for cancer detection and therapy</b> .....	19
<b>1.2.2 Clinical applications of 5-ALA for FGS</b> .....	20
<b>1.2.3 Limitations of 5-ALA use for FGS applications</b> .....	21
<b>1.3 Mitogen-activated protein kinases (MAPK) signalling pathway</b> .....	22
<b>1.3.1 MAPK Protein Kinase Family</b> .....	22
<b>1.3.2 MAPK signaling pathway</b> .....	23
<b>1.3.2.1 JNK and p38 signaling pathway</b> .....	23
<b>1.3.2.2 ERK 1 and MEK1/2 signalling pathway</b> .....	23
<b>1.3.3 Pharmacological inhibitors for MEKs</b> .....	26
<b>1.3.4 Clinical development of next-generation MEK inhibitors</b> .....	27
<b>1.4 Study rationales</b> .....	28
<b>Chapter 2: Material and methods</b> .....	31
<b>2.1 Cell culture</b> .....	31
<b>2.2 Reagents</b> .....	36

2.2.1	Administration protocol for the MEK inhibitor U0126 .....	36
2.2.2	Administration protocol for 5-aminolevulinic acid (5-ALA) .....	36
2.3	Effects of MEK inhibition on PpIX accumulation <i>in vitro</i> .....	36
2.4	Effect of MEK inhibition on PpIX accumulation <i>in vivo</i> .....	37
2.4.1	Mouse strains and animal housing .....	37
2.4.2	Transplanted mammary tumour model (4T1) .....	38
2.4.3	Spontaneous transgenic mammary tumour model (HRAS) .....	39
2.4.4	Mammary tumour homogenization .....	39
2.4.5	Protein assay and PpIX measurement of <i>in vivo</i> tumour samples .....	39
2.4.6	Fluorescence imaging of PpIX-labelled mammary tumours .....	40
2.5	Statistical analysis .....	40
<b>Chapter 3: Results .....</b>		<b>41</b>
3.1	<b>MEK inhibition promotes PpIX accumulation in a cancer specific manner</b> 41	
3.1.1	Promotion of PpIX accumulation by MEK inhibition in human normal and breast cancer cell lines .....	41
3.2	<b>Promotion of PpIX accumulation by MEK inhibition in different types of cancer cell lines.....</b>	<b>43</b>
3.2.1	Human breast cancer cell lines.....	43
3.2.2	Human lung cancer cell lines.....	43
3.2.3	Human prostate cancer cell lines .....	44
3.3	<b>Promotion of PpIX accumulation by MEK inhibition in <i>in vivo</i> cancer models.....</b>	<b>46</b>
3.3.1	Screening of mouse cancer cell lines <i>in vitro</i> .....	46
3.4	<b>PpIX accumulation by U0126 MEK inhibition <i>in vivo</i>.....</b>	<b>48</b>
3.4.1	<i>In vivo</i> : Mouse 4T1 breast tumour model .....	48
3.4.2	<i>In vivo</i> : H-Ras transgenic mouse model .....	49
3.4.2	<i>In vivo</i> tumour imaging by PpIX fluorescence .....	53
<b>Chapter 4: Discussion .....</b>		<b>56</b>
4.1	<b>General Discussion .....</b>	<b>56</b>
4.2	<b><i>In vitro</i> experimental models .....</b>	<b>57</b>
4.3	<b><i>In vivo</i> experimental models .....</b>	<b>58</b>
4.4	<b>Possible mechanisms of PpIX accumulation by U0126 MEK inhibitor.....</b>	<b>60</b>

4.4.1	Downregulation of ABCG2 by U0126 .....	60
4.4.2	Downregulation or inhibition of FECH by U0126 .....	62
4.4.3	Reduction of cellular pH by MEK inhibition .....	63
4.5	Compounds that leads to PpIX accumulation .....	64
4.5.1	ABCG2 inhibitors .....	64
4.5.2	FECH inhibitors .....	65
4.5.3	Feasibility of MEK inhibitors for use in FGS applications .....	65
4.6	Conclusion .....	66
4.7	Future Directions.....	67

## List of Tables

<b>Table 1: Non-specific fluorescence contrast agents</b> .....	13
<b>Table 2: Tumour-specific fluorescence contrast agents</b> .....	14
<b>Table 3: Endogenous fluorescence contrast agents</b> .....	15
<b>Table 4: Human breast cell lines</b> .....	32
<b>Table 5: Human lung cell lines</b> .....	33
<b>Table 6: Human prostate cell lines</b> .....	34
<b>Table 7: Mouse cancer cell lines</b> .....	35

## List of Figures

<b>Figure 1: Principle of fluorescence emission.....</b>	<b>8</b>
<b>Figure 2: Heme biosynthesis pathway .....</b>	<b>18</b>
<b>Figure 3: Mitogen-activated protein kinase (MAPK) signaling pathways.....</b>	<b>25</b>
<b>Figure 4: PpIX accumulation by MEK inhibitor .....</b>	<b>30</b>
<b>Figure 5: Cancer specific promotion of PpIX by MEK inhibition.....</b>	<b>42</b>
<b>Figure 6: Promotion of PpIX accumulation by MEK inhibition in human breast, lung and prostate cancer cells .....</b>	<b>45</b>
<b>Figure 7: Promotion of PpIX accumulation by MEK inhibition in mouse cancer cell lines .....</b>	<b>47</b>
<b>Figure 8: Promotion of PpIX accumulation by MEK inhibition in 4T1 mammary tumour models.....</b>	<b>51</b>
<b>Figure 9: Promotion of PpIX accumulation by MEK inhibition in H-Ras transgenic mice .....</b>	<b>52</b>
<b>Figure 10: Real time visualization of PpIX accumulation by MEK inhibitor in 4T1 tumours.....</b>	<b>54</b>
<b>Figure 11: Real time visualization of PpIX accumulation by MEK inhibitor in HRAS tumours.....</b>	<b>55</b>



## List of Abbreviations

°C	degrees Celsius
µg	microgram
µM	micromolar
5-ALA	δ-Aminolevulinic acid
ABC	ATP-binding cassette
ABCG2	ABC transporter G2
ALA-D	ALA dehydratase
ALA-S	ALA synthetase
AZD6244	Selumetinib
BCA	Bicinchoninic acid
BRAF	Proto-oncogene B-Raf
Coprogen III	Coproporphyrinogen III
CPO	Coproporphyrinogen oxidase
DFX	Deferoxamine
DMEM	Dulbecco's modified Eagle's medium
DMSO	Dimethyl Sulfoxide
DNA	Deoxyribonucleic acid
EGFR	Epidermal growth factor receptor
EGFR	Epidermal growth factor receptor
ER	Estrogen-receptor-positive
ERK	Extracellular signal-regulated kinase
FAD	Flavin adenine dinucleotide
FBS	Fetal bovine serum
FDA	Food and Drug Administration
FECH	Ferrochelatase
FGS	Fluorescence guided surgery
GEF	Guanine nucleotide exchange factors

GEFs	Guanine nucleotide exchange factors
GSK	Trametinib
h	Hour(s)
HMB	Hydroxymethylbilane
HMBS	Hydroxymethylbilane synthase
IP	Intraperitoneal injection
IT	Intraumoural
JNK1/2/3	C-Jun amino (N)-terminal kinases 1/2/3
LLC	Lung cancer cell line
M	Molar
MEK	Mitogen activated protein kinase
m	Minute(s)
ml	Millilitre(s)
mM	Millimolar
mRNA	Messenger ribonucleic acid
MPR	Multi-drug resistance proteins
NADH	Nicotinamide Adenine Dinucleotide
ng	Nanogram
nM	Nanomolar
PBG-D	Porphobilinogren deaminase
PBS	Phosphate buffered saline
Pfizer	CI-1040
PpIX	Porphyrin IX
PPO	Protoporphyrinogen oxidase
Protogen III	Protoporphyrinogen
Radiotherapy	Radiation therapy
RAF	Serine/threonine protein kinase
RIPA	Radioimmunoprecipitation assay buffer

RT-PCR	Reverse transcription polymerase chain reaction
SDS	Sodium dodecyl sulfate
UCS	Uroporphyrinogen cosynthase
UROD	Uroporphyrinogen III decarboxylase
Urogen III	Uroporphyrinogen III
UROS	Uroporphyrinogen III synthase
GBM I and II	Low grade glioblastoma

## **Chapter 1: Introduction**

### **1.1 Therapeutic strategies for cancer treatment**

Cancer is a major public health problem across the globe. In the next two decades the number of new cancer cases will rise to 22 million worldwide (Siegel, Miller, and Jemal 2015). Fortunately, the cancer-associated mortality rate has declined as a result of improved cancer awareness, screening, prevention and clinical treatments. According to the Canadian Cancer Society Statistics Report (2015), as a result of cancer prevention efforts over 126,000 deaths have been avoided since 1988, when the cancer mortality rate peaked in Canada. There was an increase in survival rate from 56 % to 63 % between 1992-94 and 2006-08, considering all cancers combined in Canada ("Canadian Cancer Society," 2016). These statistics show that progress is being made to treat cancer and extend the expected lifespan of cancer patients, but much work still remains. There are several treatment methods that play a major role in cancer control, such as chemotherapy, radiotherapy and surgical removal of solid tumours; each of these options have some advantages and some disadvantages for the patient during their cancer treatment. Generally, cancer therapies are selected by the oncological team based on the type or stage of the cancer and the patient's health status ("Canadian Cancer Society," 2016).

Chemotherapy is one approach for cancer treatment that targets cancer cells with pharmaceutical drugs. Traditional chemotherapeutic agents are toxic

and target cancer cell proliferation to effectively poison cancer cells that divide rapidly, which in return would also damage normal cells that divide rapidly including: bone marrow, digestive tract and hair follicles (Raguz and Yagüe 2008). Chemotherapy may be given as a single treatment or it may be given along with other anticancer therapies. One major advantage of chemotherapy is wide distribution of the drug through the whole body, with the potential to target cancer cells that have metastasized away from the primary tumour site.

Chemotherapeutic drugs are sometimes combined to manage tumour cell populations that have heterogeneous features, with the intent of dose reduction for single agents to reduce the side-effects (Gamelin et al. 2008). Newer chemotherapeutic combinations include more targeted drugs that are directed to a specific feature of the cancer cell, such as a membrane bound receptors or cell surface antigens, as opposed to the cell replication machinery. For instance, specific antigens or receptors expressed on tumour cells can be used to develop targeted prodrugs by conjugating anti-cancer drugs to monoclonal antibodies or ligands. These prodrugs can be targeted selectively to tumours without harming normal cells and release the more toxic drug inside or outside the tumour cell, leading to cancer cell death (Singh, Palombo, and Sinko 2008). Targeted therapies are generally more selective and less toxic than traditional chemotherapy, primarily because the mechanisms of targeted therapies differ from the more traditional cytotoxic chemotherapies (Gerber 2008).

Though chemotherapy has been proven to be one of the most effective cancer treatment methods for several types of cancer, it comes with various short and long-term side effects. According to the Canadian Cancer Society symptoms such as nausea, vomiting, loss of appetite, constipation or diarrhea are common short-term side effects experienced by chemotherapy patients (“Canadian Cancer Society,” 2015). In the long-term, the first round of chemotherapy might not be curative due to the emergence of recurrent disease. The quality of life after chemotherapy is another critical factor for a patient’s health. Side effects related to chemotherapy may appear months after treatment has ended, with heart or kidney problems and lung tissue damage as some of the common long-term side effects (“Canadian Cancer Statistics” 2015). For instance, the survivors of breast cancer are at significantly increased risk of death caused by cardiovascular complications, including heart failure, hypertension and arrhythmias (Bodai and Tusó 2015). Traditional chemotherapies also have mutagenic potential, which is not a particularly good choice for childhood cancer patients, since the treatment comes with an increased risk of secondary cancers due to chemotherapy (Maniar et al. 1991). For each patient, the choice of chemotherapy is weighed against the benefits and risks, in accordance with the patient’s health, age and prognosis.

Radiation therapy (radiotherapy) is another method that delivers cancer-killing doses of ionizing radiation precisely to one particular location. Unlike chemotherapy, the damage to the normal cells in the body is significantly

reduced with the use of localized radiation. Radiotherapy alone may be used for treatment of small tumours and is also useful to shrink large mass tumours before surgery (Silva et al. 2015). Radiation therapy is usually synergistic with chemotherapy and has been used in susceptible cancers before, during, and after chemotherapy (Ragaz et al. 1997). However, radiotherapy and chemotherapy usually require a lengthy treatment time of nearly 5–6 weeks. Several factors that influence a patient's choice for surgical interventions instead of this long course of treatment include advanced age, a long travel distance to the hospital, and socioeconomic status (Blinman et al. 2013). In addition, cancer cells within a tumour are heterogeneous and the success of chemotherapy or radiotherapy is based on cancer as a homogeneous disease with consistent features across all tumour cells (Sun and Yu 2015). Resection of the tumour by surgery is the primary treatment for most solid tumours, and if the tumour is removed completely, then the patient no longer has cancer and is ultimately "cured". Therefore, surgery is a useful strategy to overcome the challenges of tumour heterogeneity. Furthermore, since tumour resection removes as many cancer cells as possible from the body, it minimizes the population that might require further treatment such as chemotherapy or radiotherapy (Nguyen and Tsien 2013).

### **1.1.1 Fluorescence-Guided Surgery**

Surgical removal of solid tumour masses is advantageous for cancer patients, but complete removal of the tumour mass is a challenge. The presence

of residual tumour cells in the target tissue post-surgery is generally associated with increased local recurrence of tumour and a decreased overall survival rate (Frankel et al. 2013; Nguyen and Tsien 2013). The other primary goal of the skilled surgeon is to retain organ function. In the case of brain tumours, for example, the border between tumour and normal tissue may not be well-defined and the surgeon is challenged to optimize tumour removal while retaining as much normal brain tissue as possible, to optimize the patient's quality of life post-surgery. Fluorescence-guided surgery (FGS) is as a medical imaging technique that facilitates the removal of solid tumours and maximizes the precision of tumour resections. FGS proceeds in real-time during the operation with simultaneous illumination of the surgical region to excite a fluorophore molecule that is selectively accumulated in the tumour tissue, while recording the fluorescence emissions through specialized imaging filters or lenses (Mondal et al. 2014). Although cure is the primary goal of cancer surgery, preservation of important structures during surgery such as nerves, blood vessels, ureters and bile ducts is equally crucial in achieving optimal outcome (Nguyen and Tsien 2013). Moreover, chronic post-surgical pain caused by nerve damage may lead to loss of function and certainly reduces the patient's quality of life (Burke and Shorten 2009). Therefore, it is important for a surgeon to be able to see structures for an accurate resection and prevent damage to normal tissues and organs; for this purpose, FGS is a valuable strategy to support both desired outcomes of tumour surgery.



### 1.1.2 Properties of Fluorophores

The full potential of FGS for optimal tumour removal relies on the chemical properties of the contrast molecules used to discriminate the tumour from normal tissues (Allison 2015). As a chemical class, fluorophores have the unique property of energy absorption leading to electron excitement, followed by electron relaxation and energy release in the form of light. Generally, the light emission is of lower energy (longer) wavelength than the excitation wavelength, which represents a shift on the visible colour spectrum (Allison 2015). Figure 1 illustrates the pattern of light absorption, electron responses in the fluorophore and the wavelength output. Due to exposure of excitation light, the electron of a specific fluorophore reaches a higher energy level or electron shell (e.g. S1 or S2) above the ground state (S0). The excited electrons primarily relax at S1 level and then return to their S0, where energy is released as fluorescence (Lakowicz 2006). The time interval that fluorophore electrons stay in the excited state before returning to the ground state is known as the fluorescence lifetime, while the number of photons emitted as a proportion of the photons absorbed is known as the quantum yield of the fluorophore. The quantum yield can be affected by the environment of the fluorophore. This is particularly important for FGS applications when the fluorophore is located under the tissue surface, since the excitation light must travel through tissues to reach the fluorophore. Fluorescence emissions can also be influenced by several factors, such as scattering, absorption, angle of light and tissue surface, and only some of the emissions are on the visible spectrum and detectable by the human eye (Lakowicz 2006). The

most important intrinsic fluorophore characteristics to consider for FGS are the fluorescence lifetime, excitation and emission spectra and quantum yield, to achieve bright, tumour-specific fluorescence that is informative for the surgeon in real-time.

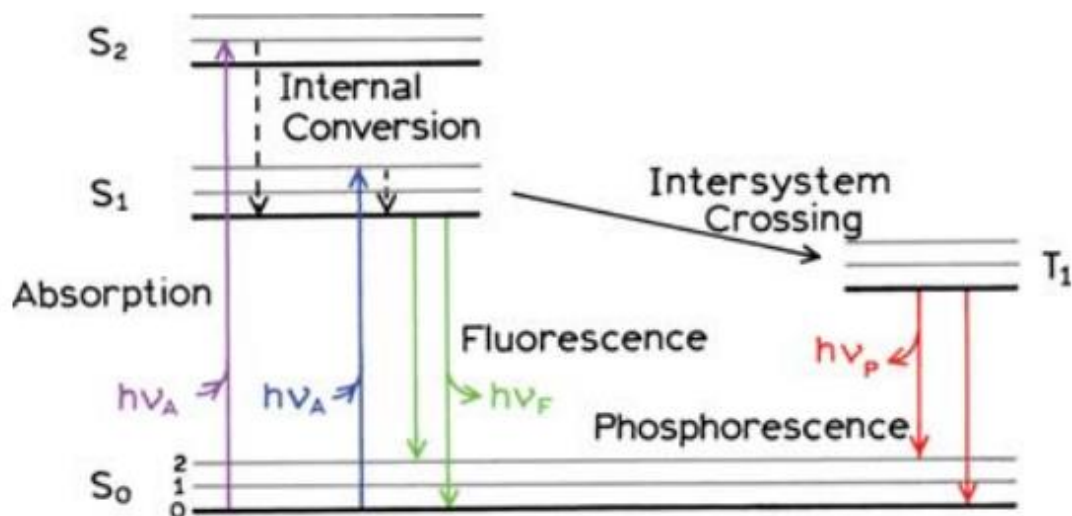


**Figure 1: Principle of fluorescence emission**

$S_0$  represent the singlet ground and  $S_1$  and  $S_2$  are the first and second electronic levels. The dashed lines at each electronic level represent the vibrational energy levels. With Permission" form springer science (Lakowicz 2006)

### **1.1.3 Basic features of Fluorescence-guided surgical practice**

There are several factors that require consideration when using fluorescence detection in the operating room or other clinical settings: the selectivity of a drug to target tumour and not normal tissue, the quantum yield of the fluorophore, representing a significant difference in fluorescence emissions between tumour and normal tissue and the ease of integration into surgical practice (Sevick-Muraca & Rasmussen,2014). Fluorescence detection of tumour margins is meant to facilitate the surgical process without introducing too much additional complexity to the operating procedures (Gioux, Choi, and Frangioni 2010). For the patient, the administered drug should be easily administered and have amphipathic properties in order to travel in the bloodstream and reach the tumour blood supply, it should be safe and not harmful for other organs or normal tissues. Ideally, the drug should also have a short life time in the body with rapid excretion or metabolism after administration (Allison 2015).

### **1.1.4 Fluorescence contrast agents**

FGS uses fluorophore in tissue, both exogenous and endogenous, to distinguish between normal and abnormal tissues. Fluorophores used in surgical applications can be divided into two main groups. They are either endogenous to tissues, or they can accumulate following administration of an exogenous compound.(Allison 2015).

#### **1.1.4.1 Exogenous fluorescence**

Exogenously administered fluorescent contrast agents generally have higher fluorescence yield compare to endogenous fluorescent agents, such that real-time imaging and detection is facilitated (Ramanujam, 2000).

There are two groups of fluorescent molecules applied to surgical procedures for solid tumours, non-specific and specific agents.

##### **1.1.4.1.1 Non-specific fluorescence contrast agents:**

These fluorophores are not tumour specific, but are designed to target rapidly proliferating tissues such as tumours or wounds, and therefore can be beneficial for FGS in certain situations. These agents are available commercially and are considered safe for clinical use. Some well-known agents in this category are Indocyanine Green, Fluorescein, and Lugol's Iodine (Table 1).

##### **1.1.4.1.2 Tumour-specific fluorescence contrast agents:**

These agents are more specifically concentrated in tumours relative to normal tissues; however the mechanism behind this phenomenon still is unknown (Huang, 2005, Matsui et al., 2010). Some of the well-known agents in this group are Photofrin, Foscan, Verteporfin (Table 2).

#### **1.1.4.2 Endogenous fluorescence**

Endogenous metabolites of the human body have fluorescent properties; natural emission of light by these structure is called autofluorescence. The most commonly observed autofluorescent molecules are: Flavin Adenine Dinucleotide

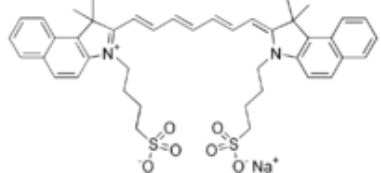
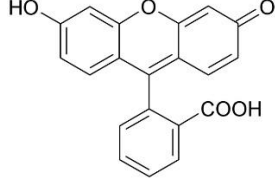
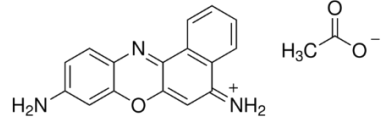
(FAD), porphyrins and intracellular Nicotinamide Adenine Dinucleotide (NADH) (Table 3). The major benefit of using autofluorescence contrast is that the patient does not need to take drugs, which prevents complications such as toxic accumulation in the kidneys and liver, or allergic reactions. However, weak quantum yield and scarcity of endogenous fluorophores limit their use in FGS imaging applications. In addition, it is difficult to use endogenous contrast in a specific manner such as distinguishing tumour from normal tissue. Due to these limitations, researchers have developed techniques to enhance endogenous fluorescence (Marcu et al.2004).

In exogenously induced fluorescence, accumulation of fluorescent molecules in tissue is either from administration of the fluorophore itself or from administration of a compound that acts as a precursor to a fluorescent molecule in a cellular pathway (Borisova et al. 2013).

$\delta$ -Aminolevulinic acid (5-ALA) is an indirect photosensitizer which promote the production of PpIX in the cells and has attracted a great attention from all over the world. Since 2007 5-ALA has been approved for clinical use in Europe. In Canada, USA, and Australia it has been tested for clinical trials. Exogenous administration of ALA overrides the heme biosynthetic pathway, resulting in increased production and accumulation of a naturally occurring fluorescent porphyrin IX (PpIX). By using proper fluorescence detection instrumentation the clinician or researchers are able to detect PpIX. 5-ALA can be used for both FGR which allow for fluorescence and Photodynamic therapy (PDT). When

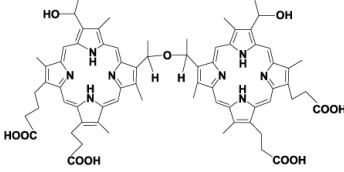
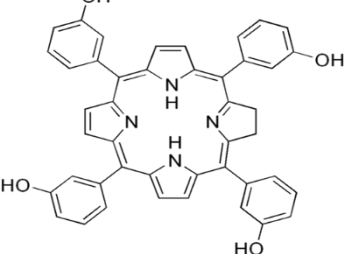
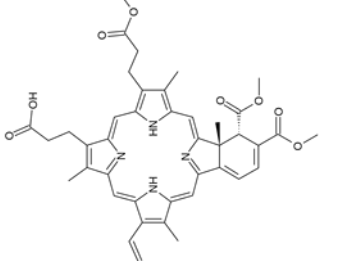
photosensitizers are exposed to a specific wavelength of light, they produce singlet oxygen that kills tumour cells (Collaud et al. 2004).

**Table 1: Non-specific fluorescence contrast agents**

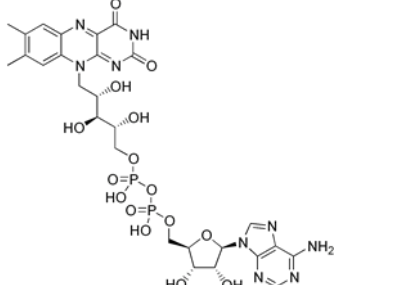
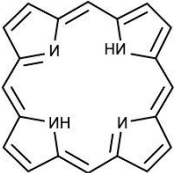
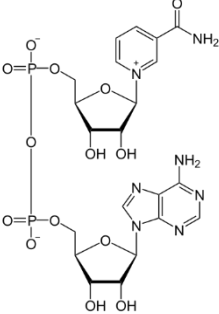
Name	Chemical Structure	Application	Excitation (nm)	Emission (nm)	Reference
Indocyanine green		lymph node status with malignant tumours	600-900	750-950	(Hirche et al. 2010)(Kraft and Ho 2014)
Fluorescein		label and track cells of interest	494	512	(Moore and Peyton1948)
Violet Acetate		Nissl staining of brain paraffin and spinal cord section. Stain RNA blue, highlight important structural features of neurons	540	625	(McDaniel and Tucker 1992)



**Table 2: Tumour-specific fluorescence contrast agents**

Name	Chemical Structure	Application	Excitation (nm)	Emission (nm)	Reference
Photofrin	<p><i>b) Photofrin<sup>®</sup></i></p>  <p><i>Esquema 2. Medicamento Photofrin<sup>®</sup></i></p>	Bladder cancer, esophageal cancer, on-small cell lung cancer	615	500	(Wezgowiec et al. 2013)
Foscan		Squamous cell carcinoma of the head and neck	420	652	(de Visscher et al. 2013)
Verteporfin		Abnormal blood vessels	436	690	(Shao et al. 2015)

**Table 3: Endogenous fluorescence contrast agents**

Name	Chemical Structure	Application	Excitation (nm)	Emission (nm)	Reference
Flavin Adenine Dinucleotide (FAD)		Monitor disease progression or aid in diagnosis.	450	515-520	(Sivabalan et al, 2010)
Porphyrins		Differentiate tumour from normal tissue during the surgery	405	635	(Peng et al. 1997)
Nicotinamide Adenine Dinucleotide (NADH)		Live imaging of different organs, Commonly used in neurosurgery to label normal from tumour tissue	340	460	(Pogue et al. 2010)

## 1.2 PpIX is an intermediate of the heme biosynthesis pathway

Heme is an essential molecule synthesized in all cells of human, animals, fungi, plants and some bacteria. The heme biosynthesis pathway consists of eight steps across different cellular compartments (Figure 2). In eukaryotes, the biosynthesis pathway is located partly in the mitochondria and partly in the cytosol. The first step of the heme biosynthesis pathway is the synthesis of 5-ALA from the amino acid glycine and succinyl CoA by ALA-synthase (ALAS) on the inner mitochondrial membrane. In the second step, 5-ALA is transferred to the cytosol where porphobilinogen (PBG) will be formed when 2 molecules of 5-ALA are condensed by metalloenzyme 5-aminolevulinate dehydrase (ALAD), also known as porphobilinogen synthase (PBG-D) (Pogue et al. 2010). In the third step, PBGs are combined by porphobilinogen deaminase and uroporphyrinogen III co-synthase in the cytosol. Next, hydroxymethylbilane (HMB) is generated by the condensation of 4 molecules of PBG (Bung et al. 2014) ; this step is catalyzed by porphobilinogendeaminase (PBGD), which is also known as hydroxymethylbilane synthase (HMBS). Porphobilinogen molecules lose their amino acids leading to the formation of a linear tetrapyrrole, which then cyclizes to form cyclic uroporphyrinogen III by uroporphyrinogen III synthase (UROS). Decarboxylation of uroporphyrinogen III by uroporphyrinogen III decarboxylase (UROD) leads to coproporphyrinogen III. Further decarboxylation and oxidation occurs by coproporphyrinogen oxidase in the mitochondria to form PpIX. The final step in heme synthesis involves insertion of an iron (II) ion into PpIX by ferrochelatase to produce heme. In contrast to

PpIX, heme has no fluorescence or photosensitizing activity (Sandanaraj et al. 2010), while PpIX has received a lot of attention since it has intense fluorescent properties useful for tumour-selective FGS (Stummer et al. 2000).

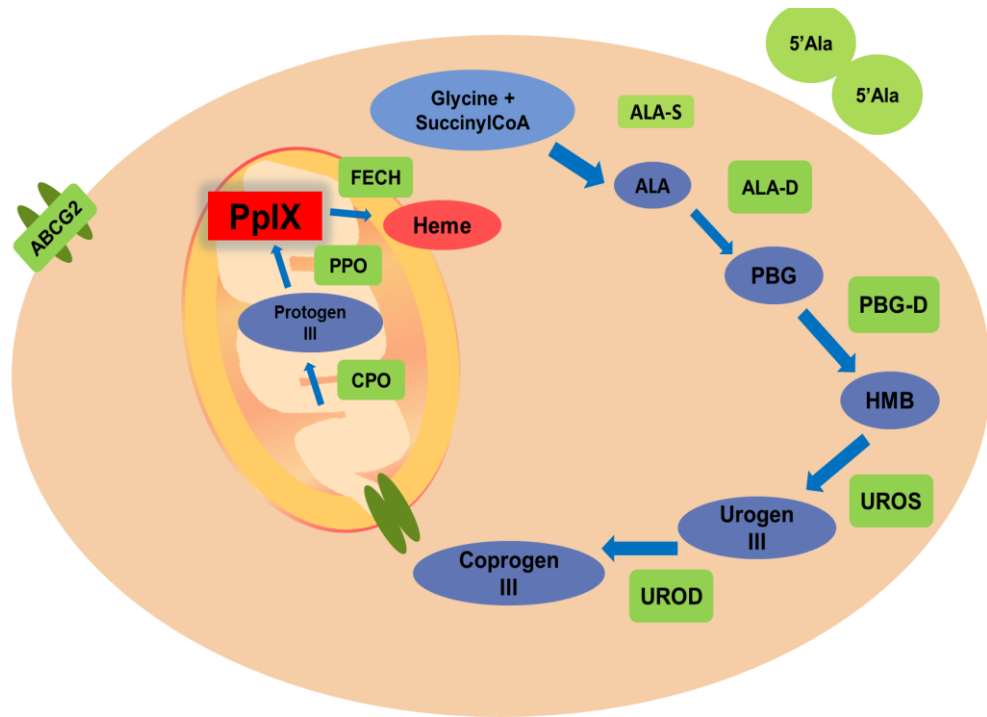


**Figure 2: Heme biosynthesis pathway**

5-ALA is a non-fluorescing substance and precursor of heme biosynthesis. Exogenous administration of 5-ALA leads to accumulation of the strongly fluorescing PpIX in tumour tissue. Several factors and enzymes are involved in this complex pathway.

ALA-D: ALA dehydratase; ALA-S: ALA synthetase; Coprogen III: coproporphyrinogen III; CPO: coproporphyrinogen oxidase; FECH: ferrochelatase; HMB: hydroxymethylbilane, PBG-D: porphobilinogen deaminase; protogen III: protoporphyrinogen; PPO: protoporphyrinogen oxidase; Urogen III: uroporphyrinogen III; UCS: uroporphyrinogen cosynthase, UGD: uroporphyrinogen decarboxylase.

### **1.2.1 5-Aminolevulinic Acid (5-ALA) for cancer detection and therapy**

Since 1992, recognition of 5-ALA induced PpIX accumulation as a common feature of epithelial tumours has led to the development of specific instrumentation to detect PpIX with endoscopic and open surgery FGS methods (Valdés et al. 2011). For example, 5-ALA has been used as a biomarker for distinguishing normal tissue from tumour tissue with success in cases of high grade glioblastoma and bladder cancer (Lau et al. 2015). For human use, 5-ALA is dissolved in water and administered orally within 1 h prior to visualization (Morimoto et al. 2014). However, in pre-clinical studies involving animal models, administration of the drug via injection is the ideal route, since 5-ALA has an unpleasant taste and is difficult for animals to ingest (Stummer et al. 1998; Lin et al. 2001).

The mechanism underlying the selective accumulation of PpIX upon 5-ALA administration in tumours is still not fully understood. The net cellular accumulation of PpIX stimulated by 5-ALA treatment is dependent on several factors such as 5-ALA uptake, the rate of PpIX synthesis, the rate of iron incorporation to produce non-fluorescent heme and the rate of PpIX efflux through different transporters to the cell microenvironment (Kobuchi et al. 2012). Several studies have indicated that the elimination of PpIX from cells is carried out by the ATP-binding cassette (ABC) transporter G2 (ABCG2), which is a multi-drug resistance-associated protein (Fujita et al. 2016; Imai et al. 2009; Yamamoto et al. 2013). Furthermore, tumours with a high metabolic rate have a

decrease in the cellular iron supply which reduces PpIX conversion to heme, leading to PpIX accumulation (Pichlmeier et al. 2008; Zhou et al. 2005). For FGS, cellular factors influencing the net balance of rapid PpIX accumulation are most significant to identify tumour foci.

### **1.2.2 Clinical applications of 5-ALA for FGS**

The dosing of 5-ALA to induce PpIX is a simple procedure for the cancer patient. In brief, a few h before the surgery, 5-ALA, 20 mg/kg per body weight (BW) is administered orally to the patient, which leads to PpIX accumulation selectively in their solid tumours (Loh et al. 1993). By using violet-blue light with excitation of 405 nm, tumours can be visualized in real time by emitted fluorescence at 635 nm, turning the tumour tissue into a red-pink color relative to the blue illumination field of normal tissues. This high colour contrast assists the surgeons with fluorescent guidance during the tumour resection (Stummer et al. 2000). 5-ALA derivatives have been used to stimulate the PpIX-fluorescence as a surgical biomarker for several types of cancer in clinics all around the world. The European Union allows photodynamic detection of cancer of the bladder, brain, and skin (Millon et al.2010). For instance, FGS approach was validated by pathologist, in terms of tumour/normal tissue boundaries in malignant glioma resection using 5-ALA stimulated PpIX for FGS (Pichlmeier et al. 2008). In the United States, 5-ALA has been applied in clinical studies and the FDA has approved it for use on skin cancer (Millon et al.2010). The potential for 5-ALA in FGS is great; however, global use to improve patient outcomes is hampered by

several factors, primarily related to variation in the net PpIX accumulation profile of different tumour classes (Silva et al. 2015).

### **1.2.3 Limitations of 5-ALA use for FGS applications**

Although 5-ALA allows surgeons to more accurately distinguish tumour tissue from normal tissue, there are some limitations to using 5-ALA as a single contrast stimulus. Even though significant success was observed for malignant glioma resections, inconsistencies in fluorescence contrast using 5-ALA have also been reported (Stummer et al. 2000). For example, some tumours do not fluoresce in patients after treatment with 5-ALA (Moiyadi, Syed, and Srivastava 2014). One hypothesis for a lack of consistent response might relate to the cancer subtype, with 5-ALA induced PpIX fluorescence being more consistent and reliable in high-grade glioblastoma, while in low grade glioblastoma (GBM I and II) there is no significant PpIX fluorescence accumulation and therefore 5-ALA cannot be used as a biomarker for fluorescence assisted surgery (S. Zhao et al. 2013). Furthermore, the fluorescence quality plays a major role in surgical outcomes. According to a study reporting two types of fluorescence: dense and bright fluorescence vs unclear fluorescence. Unclear fluorescence leads to the potential for unidentified tumour tissue that is missed during FGS (Metildi et al. 2012). In terms of short-term disadvantages, one other outcome of 5-ALA loading during the surgery is short term photosensitivity in the skin and the eyes may become very sensitive to light (Inoue et al. 2016). Therefore, it is very important to protect the eyes and skin during this time and avoid bright lights and direct



sunlight that could lead to skin irritation or eye damage (“Photodynamic Therapy” 2016). To overcome these limitations, experimental therapeutic research to enhance the sensitivity and specificity of PpIX-mediated FGS for tumour detection could lead to better patient outcomes with more complete resections and reduced side effects (Valdés et al. 2011; Y. Zhao and Adjei 2014). For this purpose, a better understanding of the mechanism of tumour PpIX accumulation is warranted. Since PpIX accumulation is a generalized property of many tumour types such as skin, bladder and brain. One approach is to investigate associations with other commonly disrupted signalling pathways in a majority of human cancers. One prominent example is the high frequency of activating mutations of the Ras intracellular signalling protein, a pro-oncogenic member of the Mitogen-activated protein kinase cascade that is found in approximately 30% of all human cancers (Roberts and Der 2007).

### **1.3 Mitogen-activated protein kinases (MAPK) signalling pathway**

#### **1.3.1 MAPK Protein Kinase Family**

Kinase is an enzyme that catalyzes the transfer of phosphate groups from high energy molecule (such as ATP) to specific substrates. This process is known as phosphorylation. MAPKs are a family of kinases that participate in signal transduction pathways responsible for regulating gene expression, motility, metabolism, survival, apoptosis and differentiation (Chakraborty et al. 2013). Some of the kinases that comprise the MAPKs family include the serine/threonine protein kinase (Raf), mitogen-activated protein/extracellular

signal-regulated kinase (MEK), the extracellular signal regulated kinases (ERK) kinase family, c-Jun amino (N)-terminal kinases 1/2/3 (JNK1/2/3), and the p38 map kinase family isoforms ( $\alpha, \beta, \lambda, \delta$ ) (Montagut and Settleman 2009)(Figure 3).

### **1.3.2 MAPK signaling pathway**

Activation of the MAPK signalling pathway is via signal initiation which depends on several factors such as growth factors, hormones, and cytokines and through the Ras and Rho families of small GTPases (Roberts and Der 2007). Three MAPK families have been distinguished: Jun kinase (JNK/SAPK), p38 MAPK and extracellular signal-regulated kinase (ERK)(W. Zhang and Liu 2002).

#### **1.3.2.1 JNK and p38 signaling pathway**

The JNK family of MAPKs, which are known as stress activated protein kinases, are activated by stress stimuli such as environmental stress, radiation and growth factors. Members of p38 family of MAPKs are primarily activated by stress stimuli, but also during engagement of various cytokine receptors by their ligands. The function of p38 kinases is required for various activities, including signal transduction mediator and regulation of apoptosis and cell cycle arrest, cell differentiation, as well as cytokine production and inflammation (Dhillon et al. 2007).

#### **1.3.2.2 ERK 1 and MEK1/2 signalling pathway**

Stimuli such as growth factors, cytokines and extracellular mitogens activates MAPK signalling cascades. Upon activation, MAPKs send signals to several intracellular targets and leads to binding of diverse collection of growth

factors receptors including epidermal growth factor receptor (EGFR). Following activation, MAPKs recruit guanine nucleotide exchange factors (GEFs) to the plasma membrane where it activates RAS GTPases by conversion of GDP-bound RAS to active GTP-bound RAS. RAF kinases are activated and recruited to the membrane by activated RAS. Subsequently, RAF activates MEK kinases. MEK1/2 are dual specificity kinases that catalyse the phosphorylation events of ERK1/2 at both tyrosine and threonine residues. ERK1/2 are the only known physiological substrate of MEK1/2. When ERK is phosphorylated it can translocate to the nucleus where it generates multiple phosphorylation and activates numerous transcription factors and other kinases. Activated ERK1/2 catalyse many events such as mitosis, cell differentiation, motility, metabolism, angiogenesis and apoptosis.

Mutation in components of the ERK signalling cascade are seen in approximately 30 % of all human cancers (Cargnello and Roux 2011). Extensive research has established that MEK1 and MEK2 play critical roles and contribute to tumourigenesis (Dhillon et al. 2007). In addition, proto-oncogene B-Raf (BRAF) mutations have been recognized in a narrower range of malignancies (Oikonomou et al. 2014). Therefore, the MEK pathway is widely studied and various drugs targeting this pathway have been generated for cancer therapy, as a strategy to inhibit autocrine signalling pathways that support tumour cell survival (Y. Zhao and Adjei 2014).

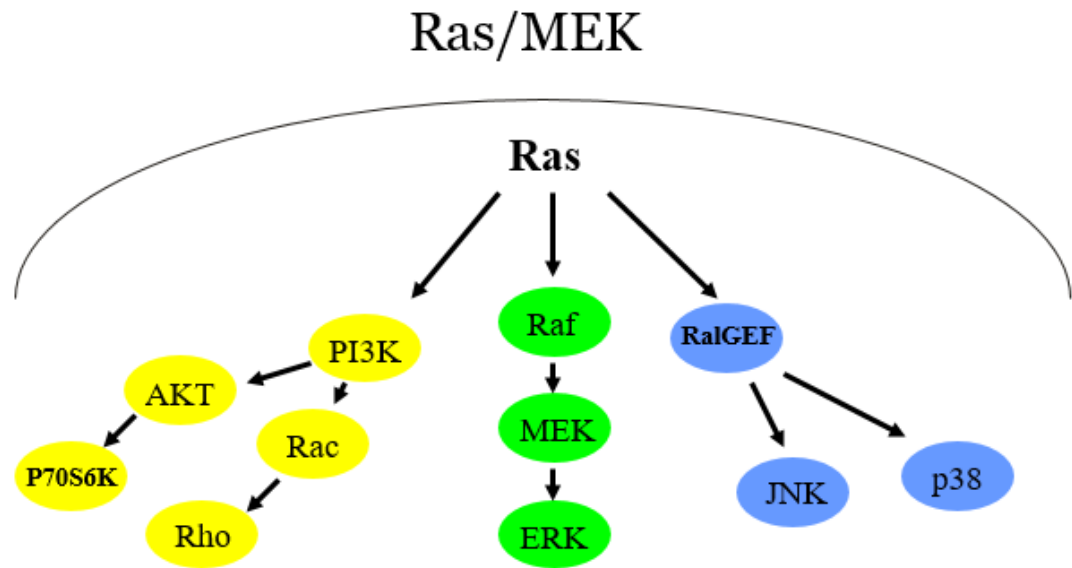


**Figure 3: Mitogen-activated protein kinase (MAPK) signaling pathways.**

MAPK signaling pathways are activated by extracellular or intracellular stimuli, upon which they activate other intracellular signaling pathways. Activated MAPKs phosphorylate numerous substrate proteins including transcription factors, resulting in regulation of a variety of cellular activities including cell proliferation, differentiation, migration, and apoptosis. The mammalian MAPK family includes ERK, p38, and JNK. In the ERK signaling pathway, ERK1/2 is activated by MEK1/2, which is activated by Raf. Raf is activated by the Ras GTPase, whose activation is induced by RTKs such as the epidermal growth factor receptor.

### 1.3.3 Pharmacological inhibitors for MEKs

Since MEK1 and MEK2 have crucial roles in tumourigenesis, including inhibition of apoptosis and promotion of cellular invasion and proliferation, several specific and highly potent MEK1/2 combination inhibitors have been developed, some of which are already assessed in clinical studies. PD98059 and U0126 were the first MEK inhibitors developed and potently inhibit MEK1 and MEK 2 in a variety of cell types. PD098059 inhibits the activity of MEK1/2 *in vitro* and *in vivo* by stabilizing the inactive conformation of MEK, and as a result, inhibits cell proliferation and induces apoptosis in solid tumours (Moon et al. 2007). U0126 is a small, non-ATP competitive molecule that appears to inhibit the activation of MEK through Raf, and as a result, also inhibits the downstream phosphorylation of ERK (Duncia et al. 1998). Through inhibition of MEK, U0126 blocks the production of various cytokines involved in inflammatory responses. For the purpose of cancer therapy, U0126 administration triggers cell cycle arrest, increased apoptosis, reduced migration potential, leading to an overall decreased tumourigenicity of cancer cells (Hawkins et al. 2008; Duncia et al. 1998). Cancer therapeutic has changed from non-specific cytotoxic agents to selective, mechanism based treatment in the past decades. MEK inhibitors, in addition to their primary anti-cancer effects, have the potential to sensitize cancer cells to other drugs (Vanneman and Dranoff 2012).

Acquired drug resistance in tumour cells is one of the main problems of chemotherapy. Tumours are heterogeneous and resistance to drugs is based on

several factors, including inhibition of apoptosis, DNA repair and increased efflux of anticancer agents out of the cells by ATP-binding cassette (ABC) transporters, also known as Multi-drug resistance proteins(MRP) (Gottesman, Fojo, and Bates 2002). Mutation of the MAPK pathway has been shown to be associated with overexpression of MRP in cancer cells (McCubrey et al. 2007a). These results suggest that MAPK pathway and drug resistance may interact with each other in cancer cells. This association of cancer cells having both features could be mechanistically related or unrelated, since they are both common features of cancer cells. However, the mechanism and involvement of the downstream MAPK pathway in mediating the ABC proteins expression remains unclear (Hoffmann et al. 2011; Chakraborty et al. 2013).

#### **1.3.4 Clinical development of next-generation MEK inhibitors**

The pharmacological structure of U0126 and PD98059, which were the first MEK kinase inhibitors developed. None of these compounds was moved to clinical trials due to their pharmaceutical limitations such as low bioavailability and distribution.

However, studies show that they are valuable tools for academic research to assist in understanding the MEK pathway. There are several other MEK inhibitors that are currently being tested in clinical trials.

The first MEK inhibitor that reached the clinical trial phase was a small-molecule CI-1040(Pfizer) which showed inhibition of tumour growth in phase I trial. However, due to the poor bioavailability of the drug and inconsistency in

phase II clinical trial the development of CI-1040 (Pfizer) was terminated. Selumetinib (AZD6244) is another MEK inhibitor. It is highly selective for MEK1 and MEK2 and is the most widely studied MEK inhibitor in the clinic. At phase II study, anti-tumour activity is observed. However, there were no significant progression-free-survival difference observed. Furthermore, studies show that Selumetinib has modest anti-tumour affect as a single agent and failed to show significant clinical activity so far. To date, there are clinical studies with combination of Selumetinib and other chemotherapies drug such as carboplatin, temsirolimus, docetaxel and PI3K inhibitors to expand the efficacy of Selumetinib.

In 2013, Trametinib (GSK) an orally bioavailable MEK1/2 inhibitor got FDA approval for metastatic melanoma with BRAF (proto-oncogene B-Raf) mutation. Trametinib prevents RAF-dependent MEK phosphorylation and activation by binding to un-phosphorylated MEK1/2 (Y. Zhao and Adjei 2014; Montagut and Settleman 2009). Trametinib is currently being studied for other types of cancer.

#### **1.4 Study rationales**

The purpose of this experimental investigation is to combine two areas of research in cancer therapeutics, with the goal to enhance PpIX fluorescence specifically in cancer cells with a combination of 5-ALA and MEK enzyme inhibitors. Previously, Hirasawa et al. made a novel observation on the interaction between the heme biosynthesis pathway and the oncogenic Ras/MEK pathway (Ema Yoshioka, Ken Hirasawa 2014). It was noted in a cancer cell culture model that MEK inhibition promotes PpIX accumulation in combination with 5-ALA

treatment and the result showed the higher PpIX accumulation with U0126 compare to PD98059 (Ema Yoshioka, Ken Hirasawa 2014). So far, there are very few compounds reported that are capable of promoting PpIX accumulation in a cancer specific manner. The combination of MEK inhibitors and 5-ALA could, therefore, promote PpIX accumulation to improve the specific fluorescent signal intensity for FGS applications, as a strategy to reduce ambiguity of tumour margins for the surgeon and to trigger PpIX loading in cancer subtypes that do not respond to 5-ALA alone.

**Hypothesis:** Pharmacological inhibition of MEK in combination with 5-ALA will promote PpIX fluorescence selectively in cancer cell culture models and animal models of cancer.

**Study Objectives:**

**Objective 1:** To determine the optimal U0126 and 5-ALA dosing paradigm to induce PpIX accumulation in a panel of human normal and cancer cell lines derived from breast, lung and prostate tissues.

**Objective 2:** To determine whether PpIX accumulation is enhanced by the combination of U0126 and 5-ALA in 2 mouse models of breast cancer.



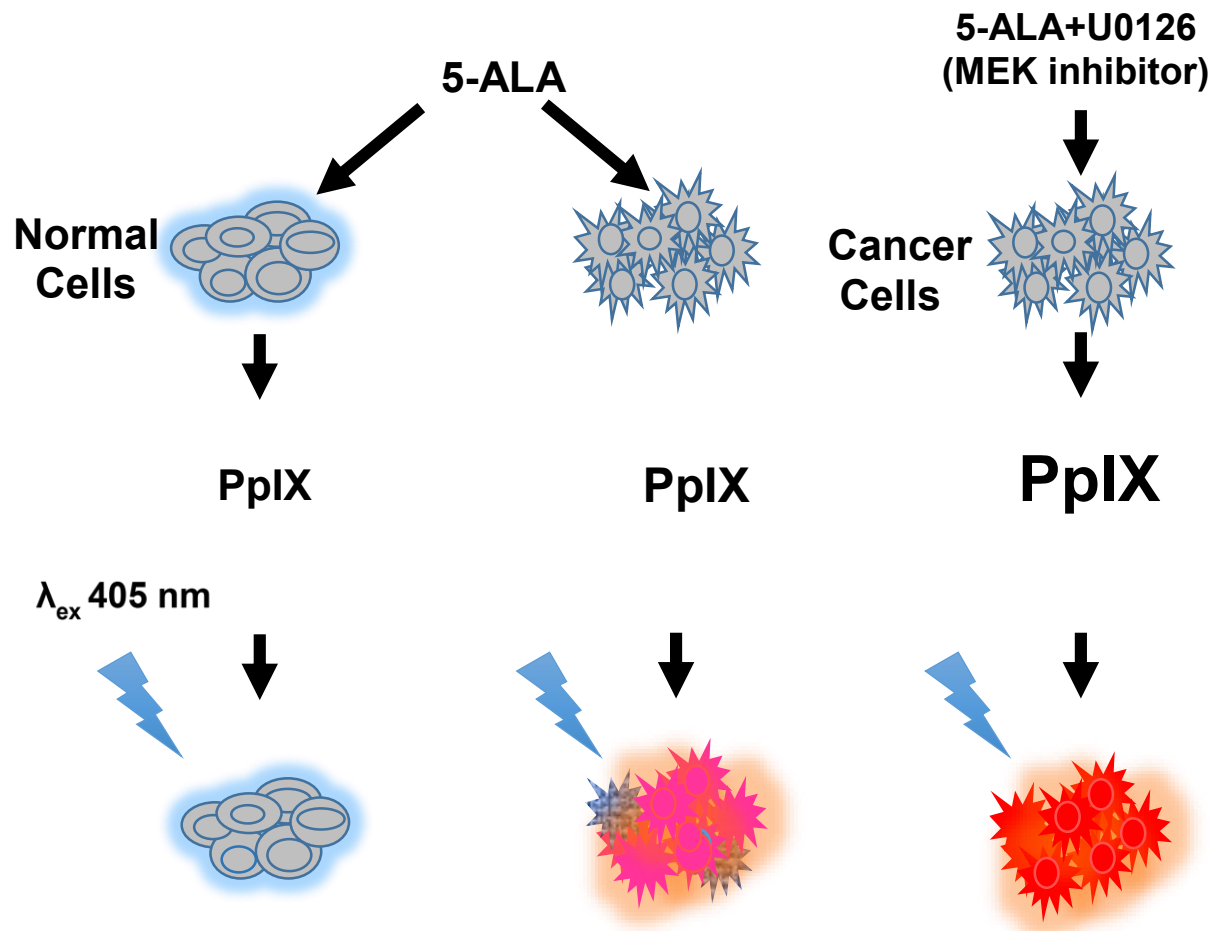


**Figure 4: PpIX accumulation by MEK inhibitor**

PpIX accumulates significantly more in cancer cells when treated with 5-ALA+U0126 (MEK inhibitor) compare to only 5-ALA treatment, therefore cancer cells emit brighter fluorescent colour which could assist the FGS for tumour detection.

## Chapter 2: Material and methods

### 2.1 Cell culture

A panel of human breast, lung and prostate normal and cancer cell lines were used in this study. All cell line were purchased from the American Type Culture Collection (ATCC). The human breast cell lines include negative (Hs578T, MDA MB 231, MDA MB 468), ER positive (T47D, MCF7, BT474) cancer cells and normal breast cells (Hs578-BST) (Table 4) The human lung cell lines include non-small lung cancer cell cells (A-549, H460, H1299,H1975) and normal lung cell cells (MRC5) (Table 5). The human prostate cell lines include androgen-independent (DU145, 22Rv1 and PC3) and androgen receptor-dependent (LnCaP) cancer cells (Table 6). 4T1 mouse mammary carcinoma cell line was obtained from Dr. Jean Marshall (Dalhousie University). Mouse Lewis lung carcinoma (LLC) and C3L5 mouse mammary carcinoma cell lines were obtained from Dr. Patrick Lee (Dalhousie University) (Table 7).

All cell lines used in this study were maintained with high glucose Dulbecco's modified Eagle's medium (DMEM) (Invitrogen, 11965-118 Canada), supplemented with 10% fetal bovine serum (FBS) (Invitrogen, 12483020, Canada), sodium pyruvate (Thermo Fisher Scientific, 11360070, Canada) and antibiotic-antimycotic mixture (Invitrogen, 15240062, Canada) (100 Units/ml penicillin G sodium) in a humidified atmosphere with 5 % CO<sub>2</sub> at a temperature of 37 °C.

**Table 4: Human breast cell lines**

<b>Breast cancer cell lines</b>	<b>Origin</b>	<b>ATTC identifier</b>	<b>Cancer subtype</b>	<b>Reference</b>	<b>Cell plating density (cells/ well, 24 well plate)</b>
<b>Hs578Bst</b>	mammary gland	HTB-125	Normal	(Hackett et al. 1977)	10×10 <sup>4</sup>
<b>BT-474</b>	mammary gland	HTB-20	Ductal Carcinoma	(Lasfargues, Coutinho, and Redfield 1978)	9×10 <sup>4</sup>
<b>Hs578T</b>	mammary gland	HTB-126	Carcinoma	(Hackett et al. 1977)	7×10 <sup>4</sup>
<b>MCF7</b>	Pleural effusion	HTB-22	Adenocarcinoma	(Sugarman et al. 1985)	4×10 <sup>4</sup>
<b>MDA-MB -231</b>	Pleural effusion	HTB-26	Medullary Carcinoma	(Brinkley et al. 1980)	4×10 <sup>4</sup>
<b>MDA-MB -468</b>	pleural effusion	HTB-132	Adenocarcinoma	(Brinkley et al. 1980)	6×10 <sup>4</sup>
<b>T-47D</b>	Pleural effusion	HTB-133	Ductal Carcinoma	(Judge and Chatterton 1983)	6×10 <sup>4</sup>

**Table 5: Human lung cell lines**

<b>Lung cancer cell lines</b>	<b>Origin</b>	<b>ATTC identifier</b>	<b>Cancer subtype</b>	<b>Reference</b>	<b>Cell plating density (cells/ well, 24 well plate)</b>
<b>MRC5</b>	Lung	CCL-171	Normal	(Jacobs, Jones, and Baille 1970)	$5 \times 10^4$
<b>A549</b>	Lung	CCL-185	Carcinoma	(Giard et al. 1973)	$3.2 \times 10^4$
<b>H460</b>	pleural effusion	HTB-177	large cell lung cancer	(Banks-Schlegel, Gazdar, and Harris 1985)	$3.2 \times 10^4$
<b>H1299</b>	Lymph node	CRL-5803	Non-small cell lung cancer	(Giaccone et al. 1992)	$4 \times 10^4$
<b>H1975</b>	Lung	CRL-5908	non-small cell lung cancer	(Phelps et al. 1996)	$4 \times 10^4$

**Table 6: Human prostate cell lines**

<b>Prostate cancer cells</b>	<b>Origin</b>	<b>ATTC identifier</b>	<b>Cancer subtype</b>	<b>Reference</b>	<b>Cell plating density (cells/ well, 24 well plate)</b>
<b>DU145</b>	prostate	HTB-81	Carcinoma	(Papsidero et al. 1981)	$5 \times 10^4$
<b>LNCap</b>	Prostate	CRL-1740	Carcinoma	(Gibas et al. 1984)	$3.2 \times 10^4$
<b>PC-3</b>	Prostate	CRL-1435	Adenocarcinoma	(Kaighn et al. 1979)	$5 \times 10^4$
<b>22Rv1</b>	Prostate	CRL-2505	Carcinoma	(Sramkoski et al. 1999)	$3.2 \times 10^4$

**Table 7: Mouse cancer cell lines**

<b>Mouse cancer cell line</b>	<b>Origin</b>	<b>Mouse strain</b>	<b>ATTC identifier</b>	<b>Cancer subtype</b>	<b>Reference</b>	<b>Cell plating density (cells/ well, 24 well plate)</b>
<b>C3-L5</b>	Breast	C3H/HeJ mice	N.A.	Carcinoma	N.A.	$5 \times 10^4$
<b>LL/2(LLC1)</b>	Lung	C57BL	CRL-1642	Carcinoma	(Bertram and Janik 1980)	$3.2 \times 10^4$
<b>4T1</b>	Breast	Balb/c	CRL-2539 Provided by Dr. Jean Marshall	Adenocarcinoma	(Pulaski et al. 2000)	$5 \times 10^4$

\* N.A. – not available

## **2.2 Reagents**

### **2.2.1 Administration protocol for the MEK inhibitor U0126**

MEK inhibitor U0126 (Cell Signaling Technology, 9903S, USA) was dissolved in DMSO (Sigma, D2650, USA) at a stock concentration of 26 mM for *in vitro* and *in vivo* studies. The stock solution was kept at -80 °C, prepared as single thaw aliquots for immediate experimental use. Cultured cells were treated with U0126 or DMSO as a diluent control at equivalent percentages to the U0126 stock.

### **2.2.2 Administration protocol for 5-aminolevulinic acid (5-ALA)**

For *in vitro* studies, monolayer cells were treated with 5-ALA (Sigma, A3785, USA) prepared as a sterile stock in serum-free Dulbecco's Modified Eagle Medium (DMEM) (Invitrogen, 11965-118, USA). The 5-ALA stock solution (500 mM) was aliquoted in small volumes and kept at -80 °C with immediate experimental use after a single freeze-thaw cycle. For *in vivo* studies, mice were injected intratumourally (it), intraperitoneally (ip) or intravenously (iv) with 5-ALA in sterile saline (0.85% NaCl, Hospira, 04888010, Canada) to achieve 200 mg/kg body weight (BW) per mouse.

## **2.3 Effects of MEK inhibition on PpIX accumulation *in vitro***

Cells were plated in 24 well plates at the cell density indicated in Table 4,5,6,7 and incubated overnight to reach 60-70 % confluence. The medium was replaced with fresh medium containing U0126 (5, 10 or 20 µM) or control vehicle DMSO (1%) as a diluent control at 1, 5, 10 or 20 h before sampling. 5-ALA (500 mM) was added to the supernatant at 5 h before sampling to achieve a final

concentration of 5mM. At the end of the desired experimental time point, cells were washed once with ice cold PBS and then lysed with 100 µl of radioimmunoprecipitation assay (RIPA) buffer (PBS pH 7.4, NP-40 1% (Sigma, MFCD02100484, USA), 0.1% sodium dodecyl sulfate (SDS) (Bio-Rad, 1610302, Canada) 0.5 % sodium deoxycholate (Sigma, 302-95-4, USA). The cell lysates were centrifuged at 11,000 x g for 10 min at 4 °C. The supernatant was transferred to a clean tube and stored at -80 °C. Cell lysates were diluted in PBS (1:30) and PpIX fluorescence was measured using a Modulus Microplate Reader (Promega BioSystems, USA), with a 450 nm excitation/635 nm emission filter.

## **2.4 Effect of MEK inhibition on PpIX accumulation *in vivo***

### **2.4.1 Mouse strains and animal housing**

Balb/c inbred female mice were obtained from Charles River Labs and transgenic mice of the FVB.Cg-Tg(WapHRAS) 69Lin Chr Y<sup>SJL</sup>/J strain (hereafter referred to as HRAS) were imported from The Jackson Laboratory (JAX Mice Stock # 002409). A unique feature of the transgenic mammary tumour model is the incorporation of the human RAS (Harvey rat sarcoma viral oncogene homolog) oncogene on to the male Y chromosome, such that male mice expressing HRAS under the mammary tissue-specific Whey acidic protein (*Wap*) promoter develop benign adenocarcinomas between 6 to 8 wks of age (Andres et al. 1987).



All mice were housed in isolated ventilated caging units with Bed-O-Cobs bedding (The Andersons Inc, Maumee OH) and suitable enrichment; cages were kept within the specific-pathogen-free barrier at the central animal care facility in the Health Sciences Centre at Memorial University of Newfoundland. Animal care protocols were approved by the Institutional Animal Care Committee, in accordance with Canadian Council on Animal Care guidelines. Mice were fed with Laboratory Rodent Diet 5010 food (27.5 % protein, 13.5 % fat, 59 % carbohydrate; OM Nutrition International, Richmond, IN) with sterile water *ad libitum*, and were housed under a 12:12 hour light/dark cycle.

#### **2.4.2 Transplanted mammary tumour model (4T1)**

Mouse mammary carcinoma 4T1 cells grown as a monolayer in a 10 cm culture dish were trypsinized and washed 3x in PBS. Female mice aged 8 wk of age were injected with  $5 \times 10^5$  cells in 100  $\mu$ l PBS subcutaneously into the right hind flank. After the development of palpable tumours (5-8 mm in diameter) in 10 days, the mice were injected intratumourly or intraperitoneally with U0126 (19 mg/kg BW in 100  $\mu$ l of DMSO/PBS) with an incubation time of 5 or 8 h prior to intraperitoneal injection with 5-ALA (200 mg/kg BW in 200  $\mu$ l saline) 2 h before sacrifice. Animals were kept in their home cages and maintained in a darkened room prior to sacrifice in consideration of 5-ALA induced photosensitivity. All animals were euthanized by CO<sub>2</sub> prior to tissue collections.

### **2.4.3 Spontaneous transgenic mammary tumour model (HRAS)**

Male HRAS mice bearing mammary tumours at approximately 3 months of age were used to determine promotion of PpIX accumulation in the tumours by U0126 treatment. Tumour sizes varied from 2-10 mm in a diameter, distributed across the mammary tumour chain, but primarily in the ventral, thoracic region. Mice were injected intraperitoneally with U0126 (50  $\mu$ M/kg) in 100  $\mu$ l DMSO (40%)/PBS for treatment group and DMSO (40 %/PBS) control group for 5 h. All animals were administered a tail vein injection of 5-ALA solution to achieve a final dose of (200 mg/ kg BW in 100  $\mu$ l saline) 1 h prior to sacrifice. Male mice were kept in their home cages and maintained in a darkened room, as described for the 4T1 subcutaneous implant tumours.

### **2.4.4 Mammary tumour homogenization**

All mice carrying implanted or spontaneous tumours were euthanized with CO<sub>2</sub> gas in a designated chamber. Tumours were then removed carefully to avoid non-tumour tissues and rinse with PBS to remove excess blood and homogenized in RIPA buffer (300  $\mu$ l). The tumour homogenate was centrifuged at 4 °C, 14,000 rpm for 10 min to collect intracellular supernatant for the protein assay and PpIX fluorescence assay, as described in Section 2.3.

### **2.4.5 Protein assay and PpIX measurement of in vivo tumour samples**

The protein concentrations of intracellular supernatant were measured using a bicinchoninic acid (BCA) protein assay kit (Thermo Scientific, PI23227,

USA) according to the manufacturer's protocol. The colorimetric quantification of BCA assay was conducted using a spectrophotometer (Beckman Coulter DU® 530) at 562 nm. PpIX fluorescence in a complementary aliquot of the matched intracellular supernatant was measured as described in section 2.3. PpIX fluorescence was standardized to protein concentration of each tumour samples. The values are shown as relative fluorescence units (RFU) per microgram of protein.

#### **2.4.6 Fluorescence imaging of PpIX-labelled mammary tumours**

Mammary tumours were illuminated with blue light (380–440 nm) generated by a D-light system (Storz GmbH, Tuttlingen, Germany) along a flexible fibre optic cable held 5-10 cm above the tissue specimen to excite PpIX fluorescence. Digital images were taken with a Canon 6D camera, fitted with a 36 mm lens and a yellow 635 nm emission lens filter.

#### **2.5 Statistical analysis**

One way ANOVA with Tukey's post-hoc test or Student's t test were performed using GraphPad Prism 4.0c software (GraphPad Software, La Jolla, CA, USA).

## **Chapter 3: Results**

### **3.1 MEK inhibition promotes PpIX accumulation in a cancer specific manner**

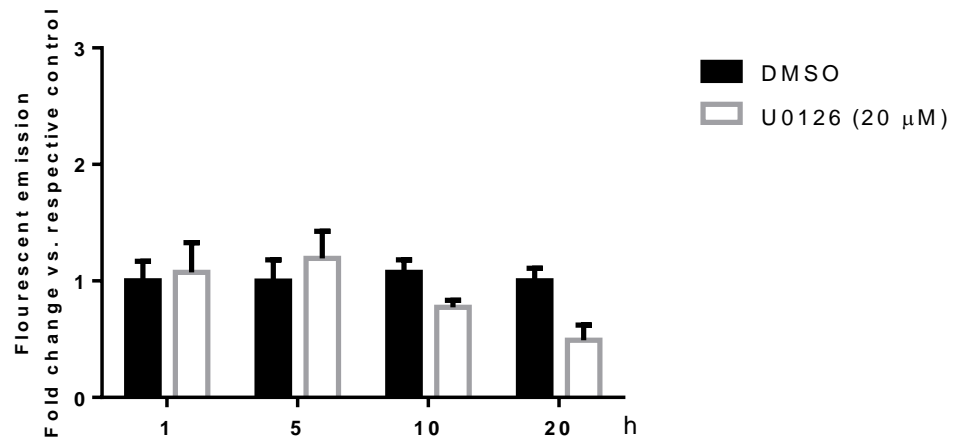
#### **3.1.1 Promotion of PpIX accumulation by MEK inhibition in human normal and breast cancer cell lines**

To determine if MEK inhibition promotes accumulation of PpIX fluorescence selectively in cancer cells, we compared the combination of a MEK inhibitor (U0126) and 5-ALA in the human immortalized breast cell line Hs578BST and the breast cancer cell line Hs578T, both of which were derived from the same patient (Hackett et al. 1977). Cells were treated with U0126 (20  $\mu$ M) or an equivalent percentage of DMSO for 1,5,10, 20 h, with 5-ALA (5mM) added 5 h prior to cell lysis. PpIX fluorescence in the lysates was measured using a fluorescent microplate reader (excitation  $\lambda$  450 nm; emission  $\lambda$  635 nm) (Figure 4A, 4B). There was no significant change in PpIX accumulation in immortalized Hs578BST breast cells treated with MEK inhibition for 1, 5, 10 or 20 h (Figure 4A). On the other hand, accumulation of PpIX fluorescence was significantly promoted in breast cancer Hs578T cells treated with 5-ALA plus U0126 for 5, 10 or 20 h, as compare to those treated with 5-ALA plus DMSO (Figure 4B). As the highest promotion was observed at 20 h after U0126 treatment, this time point was pursued in subsequent experiments.

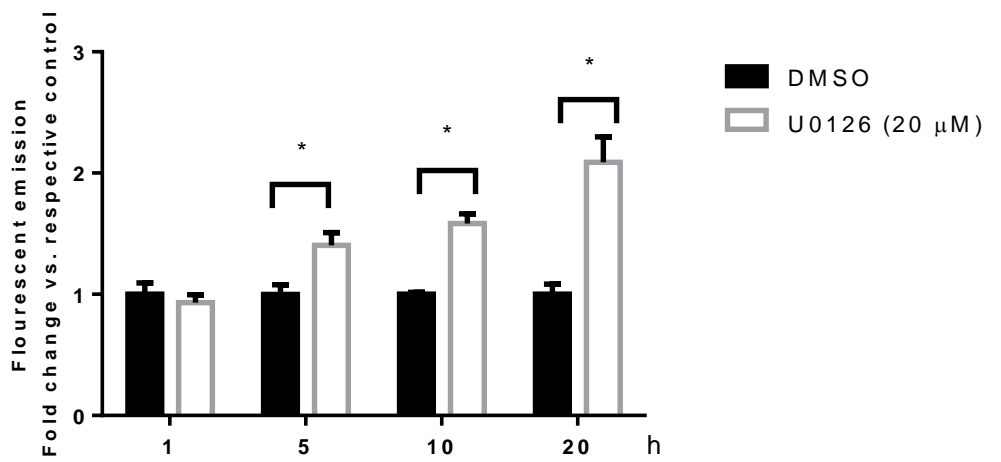
### **Figure 5: Cancer specific promotion of PpIX by MEK inhibition**

Human breast immortalized (Hs578Bst) (A) and cancer (Hs578T) (B) cells were treated with MEK inhibitor U0126 (20  $\mu$ M) or DMSO for 1, 5, 10 and 20 h, with 5-ALA (5 mM) initiated 5 h prior to cell lysis in all the treatment groups. PpIX fluorescence was measured by a fluorescent microplate reader. Minimum of 3 independent experiments were performed with quadruplicate wells for each condition. The graphs represent the average of one of the experiments. Statistical analyses performed using student's t test. \*  $p < 0.01$ .

**A** ·Hs578Bst



**B** ·Hs578T



## **3.2 Promotion of PpIX accumulation by MEK inhibition in different types of cancer cell lines.**

### **3.2.1 Human breast cancer cell lines**

To determine whether PpIX fluorescence enhancement with the combination of MEK inhibitor and 5-ALA is a generalizable phenomenon, we compared the PpIX fluorescence response of a panel of human breast cancer cells to U0126 plus 5-ALA. The human immortalized breast cell line (Hs578-BST) and 6 additional human breast cancer cell lines (BT474, Hs578-T, MCF7, MDAMB231, MDAMB468 and T47D) were treated with U0126 (20  $\mu$ M) or DMSO for 20 h, with 5-ALA (5 mM) administered to the culture medium 5 h prior to cell lysis (Figure 5A). PpIX accumulation was significantly promoted in 4 human breast cancer cell lines, Hs578T, MDA MB 231, T47D, and MCF7. On the other hand, no significant change in PpIX accumulation was induced by MEK inhibition in 2 breast cancer cell lines (MDA MB 468 and BT474) with this dosing paradigm, similar to the immortalized breast cell line Hs578-BST.

### **3.2.2 Human lung cancer cell lines**

Four human lung cancer cell lines (A549, H460, H1299 and H1975) and the immortalized human lung cell line (MRC5) were used to determine whether MEK inhibition promotes PpIX accumulation in the presence of 5-ALA (Figure 5B). PpIX accumulation was significantly promoted by MEK inhibition in 3 lung cancer cell lines treated with 5-ALA (A-549, H460 and H1299) while there was no

significant change in 5-ALA stimulated PpIX fluorescence induced by U0126 treatment in the lung cancer cell line (H1975) and the immortalized lung cell line (MRC5).

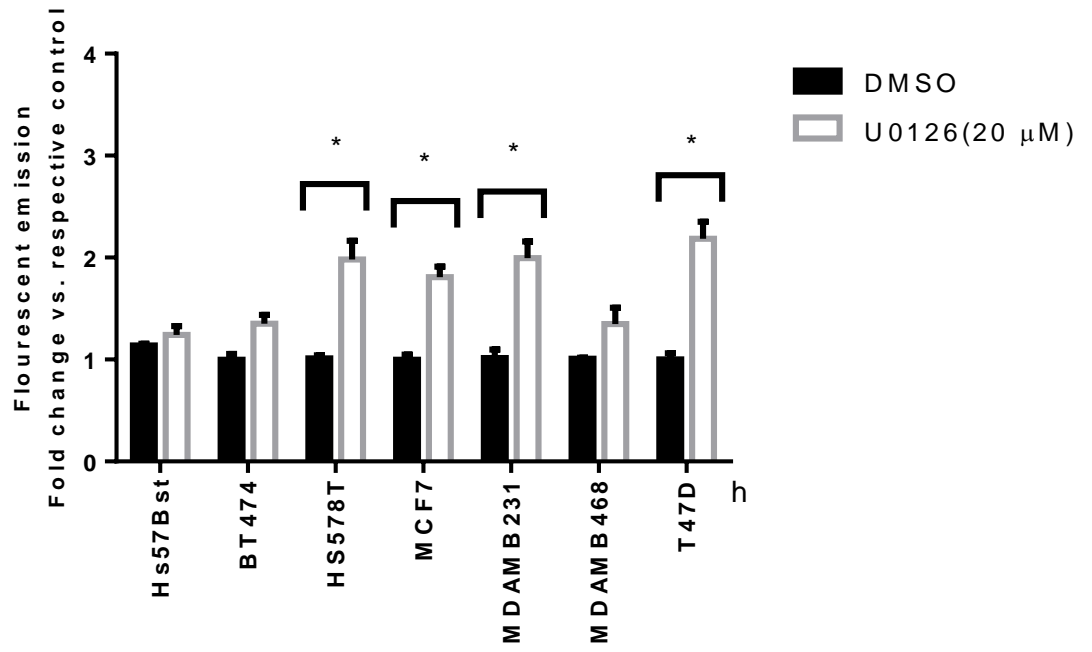
### **3.2.3 Human prostate cancer cell lines**

The promotion of PpIX accumulation by MEK inhibition plus 5-ALA was examined in 4 prostate cancer cell lines (U1456, LNCap, PC3 and 22Rv1) (Figure 5C). A significant increase in PpIX fluorescence was observed in DU145 and LnCaP prostate cancer cell lines. On the contrary, no significant change in PpIX fluorescence was observed following U0126 plus 5-ALA combined treatment in 22Rv1 or PC3 prostate cancer cells.

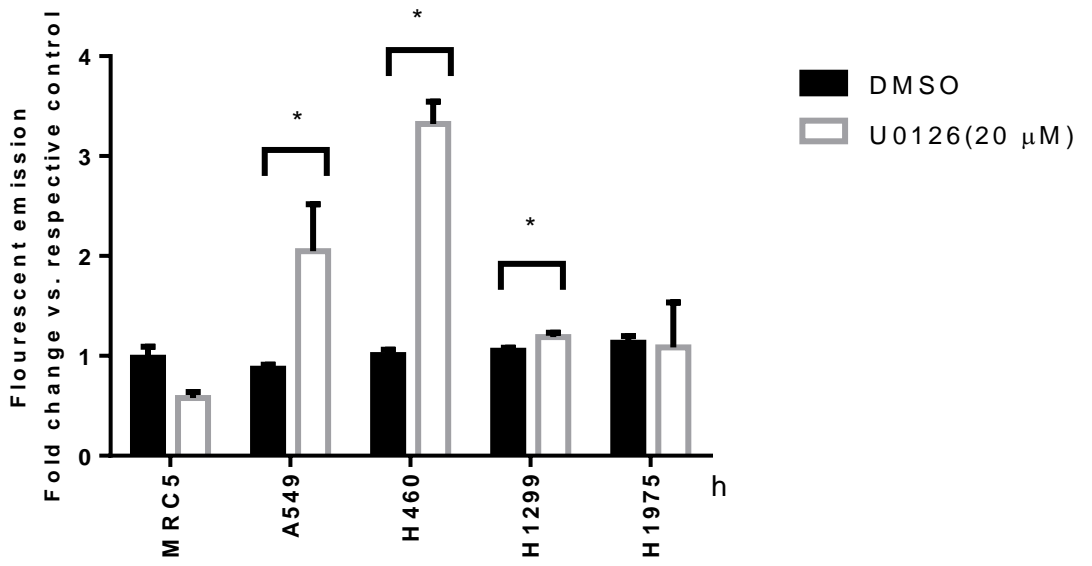
Overall, MEK inhibition increased PpIX accumulation in 4/5 breast cancer cell lines, 3/4 lung cancer cell lines and 2/4 prostate cancer cell lines, but had no effect in the 2 immortalized cell lines originating from normal human tissues. These results suggest that MEK inhibition promotes PpIX accumulation in a cancer-specific manner, but some cancer cell lines in the different subtypes evade this up-regulation in fluorescence.



A



B



C

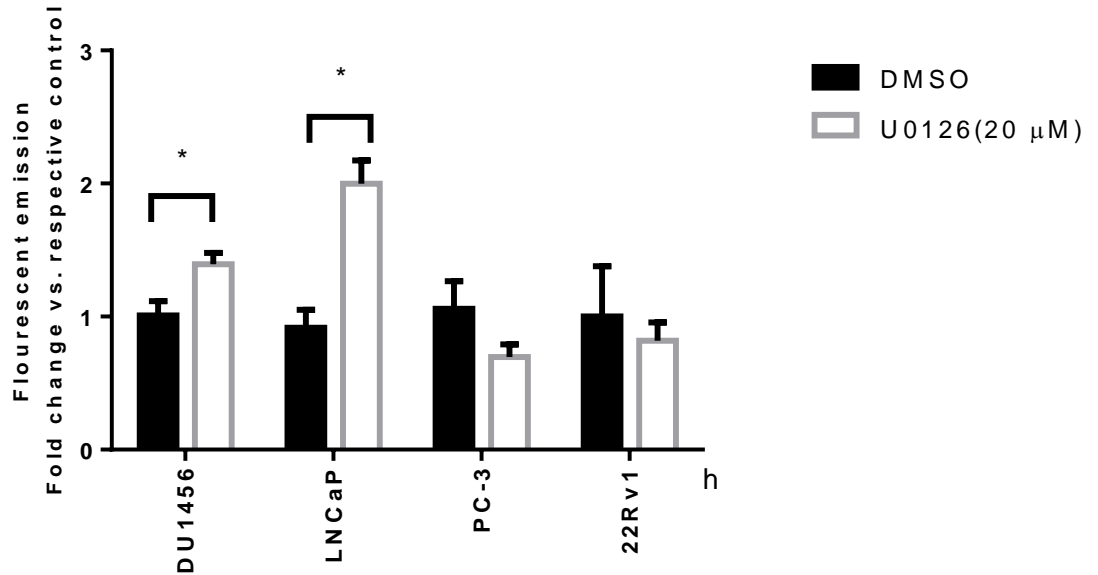


**Figure 6: Promotion of PpIX accumulation by MEK inhibition in human breast, lung and prostate cancer cells**

Human breast (A), lung (B) and prostate (C) cell lines were plated in a 24 well plate. After 24 h, the cells were treated with MEK inhibitor U0126 (20 μM) or DMSO for 20 h and 5-ALA (5 mM) for 5 h prior to cell lysis. PpIX fluorescence was measured by a fluorescent microplate reader. A minimum of 3 independent experiments were performed with quadruplicate wells for each condition. The graphs represent the average of one of the experiments. Statistical analyses performed using student's *t* test. \*  $p < 0.01$ .

### **3.3 Promotion of PpIX accumulation by MEK inhibition in *in vivo* cancer models**

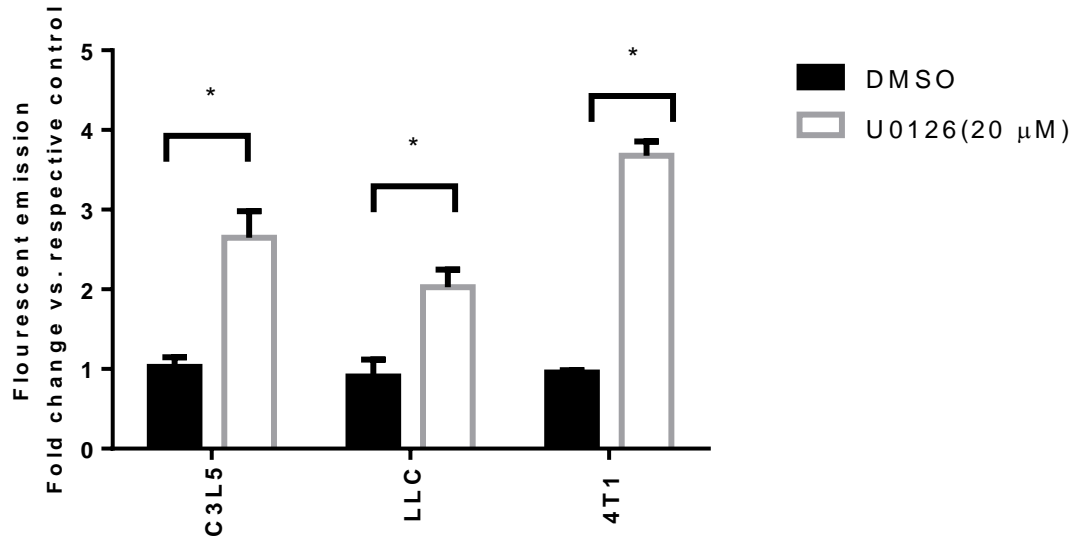
#### **3.3.1 Screening of mouse cancer cell lines *in vitro***

To conduct *in vivo* studies for the combination of MEK inhibition and 5-ALA on PpIX fluorescence, it was first necessary to identify a mouse cancer cell line in which 5-ALA-induced PpIX accumulation is promoted by U0126 treatment. Two mammary cancer cell lines (C3-L5 and 4T1) and a lung cancer cell line (Lewis lung carcinoma (LLC)) were treated with or without U0126 (20  $\mu$ M) for 20 h and then with 5-ALA (5mM) for 5 h. PpIX accumulation was significantly increased by U0126 treatment in all the mouse cancer cell lines tested (Figure 6A). Among the cell lines, 4T1 cell lines showed the highest fold change with MEK inhibition plus 5-ALA. To confirm the optimal time course for promotion of PpIX accumulation by MEK inhibition in the 4T1 line, the cells were treated with U0126 (20  $\mu$ M) for different durations (1, 5, 10 and 20 h), keeping 5-ALA exposure consistent at 5 h prior to cell lysis (Figure 6B). Similar to the human breast cancer cell line Hs578T, PpIX fluorescence was significantly promoted in 4T1 cells treated with U0126 for 5, 10 or 20 h, compare to those treated with DMSO (1 %). Based on these results, the mouse breast 4T1 tumour model was used for xenograft tumours in the animal studies, with a dosing protocol that provides U0126 several h prior to the administration of 5-ALA.

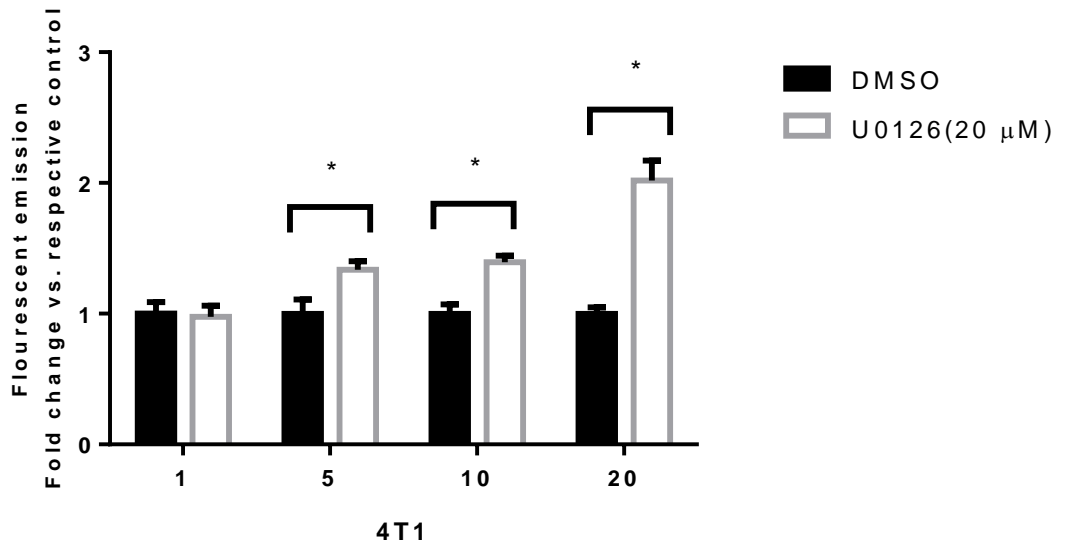
**Figure 7: Promotion of PpIX accumulation by MEK inhibition in mouse cancer cell lines**

Mouse breast cancer, C3L5 and 4T1, and mouse lung cancer, LLC, were plated in 24 well plates. (A) After 24 h, the cells were treated with MEK inhibitor U0126 (20  $\mu$ M) or DMSO for 20 h and 5-ALA (5 mM) for 5 h prior to cell lysis. (B) 4T1 cells were treated with MEK inhibitor U0126 (20  $\mu$ M) or DMSO for 1, 5, 10 and 20 h, and 5-ALA (5 mM) for 5 h prior to cell lysis. PpIX fluorescence was measured by a fluorescence microplate reader. A minimum 3 independent experiments were performed with quadruplicate wells for each condition. The graphs represent the average of one of the experiments. Statistical analyses performed using student's *t* test. \*  $p < 0.01$ .

A



B



### **3.4 PpIX accumulation by U0126 MEK inhibition *in vivo***

#### **3.4.1 *In vivo*: Mouse 4T1 breast tumour model**

To determine the efficacy of U0126 treatment on promotion of PpIX accumulation *in vivo*, 4T1 tumours were established in the hind flank of age-matched and BW-matched female BALB/c mice (n=18) by injection of  $5 \times 10^5$  cells and follow up for tumour growth over a period of 10 days. Optimal tumour size for experimental use was 5-10 mm. The mice were divided into three groups: a control group that received intra tumoural injection of DMSO/saline (40% DMSO) for 8 h (n = 6 mice), a U0126 treatment group that received intra tumoural (it) injection of U0126 (50  $\mu$ M/kg) in 250  $\mu$ l Saline/PBS for 5 h prior to sacrifice (n = 6 mice) and a U0126 treatment group that received it injection of U0126 (50  $\mu$ M/kg) in 250  $\mu$ l Salin/PBS 8 h prior to sacrifice (n = 6 mice). All three groups received 5-ALA (200 mg/kg BW) by intraperitoneal injection (ip) injection 2 h before sacrifice. The mice were sacrificed with CO<sub>2</sub> gas and the tumours were removed and homogenized. The amount of PpIX accumulation was determined as described in section 3.1.1. As shown in Figure 7A, the mean PpIX fluorescence was higher in the tumours of mice treated with 5-ALA plus U0126 for either 5 or 8 h, as compare to those treated with 5-ALA plus DMSO/saline; however, PpIX fluorescence was statistically promoted (2.5 fold) only in the tumours of mice treated with U0126 for 8 h prior to the 5-ALA injection 2 h before sacrifice.

To further confirm the results of the promotion of PpIX accumulation by it injection, it was determined whether a different route of U0126 injection, ip

injection, was also effective using the same *in vivo* tumour model. BALB/c mice bearing 4T1 tumours were again divided into three groups, as per the *in vivo* injection experiments: a control group that received ip injection of DMSO/saline (40%) (n = 6 mice), a treated group that received U0126 by ip injection (50 µM/kg) for 5 h prior to sacrifice (n = 6 mice) and a treated group that received U0126 by ip injection (50 µM/kg) for 8 h prior to sacrifice (n = 6 mice) (Figure 7B). All three groups received 5-ALA (200mg/kg BW) by intraperitoneal injection (ip) injection 2 h before sacrifice. PpIX fluorescence was significantly increased (2.5) in the tumours of mice treated with 5-ALA plus U0126 for 5 h, but not in those treated with 5-ALA plus U0126 for 8 h, as compared to those treated with vehicle control (DMSO) and 5-ALA alone.

#### **3.4.2 *In vivo*: H-Ras transgenic mouse model**

To determine whether MEK inhibition is effective to promote PpIX accumulation in spontaneous mammary tumours, the H-Ras transgenic mouse model of mammary cancer was investigated with the 5-ALA and U0126 drug combination. Mice at age 3 months with tumours ranging in size from 2-10 mm in a diameter, were divided into 2 treatment groups: a control group that received ip injection of DMSO/saline (40%) (n = 13 mice) 5 h before sacrifice, and the U0126 group received ip injection of U0126 (50 µM/Kg) (n = 13 mice) 5 h prior to sacrifice. Both groups received 5-ALA (200 mg/kg BW) by tail vein injection at 1 h before sacrifice, according to a published protocol (Dorward et al. 2005). PpIX fluorescence in the tumours was measured as described in section 3.1.1. PpIX

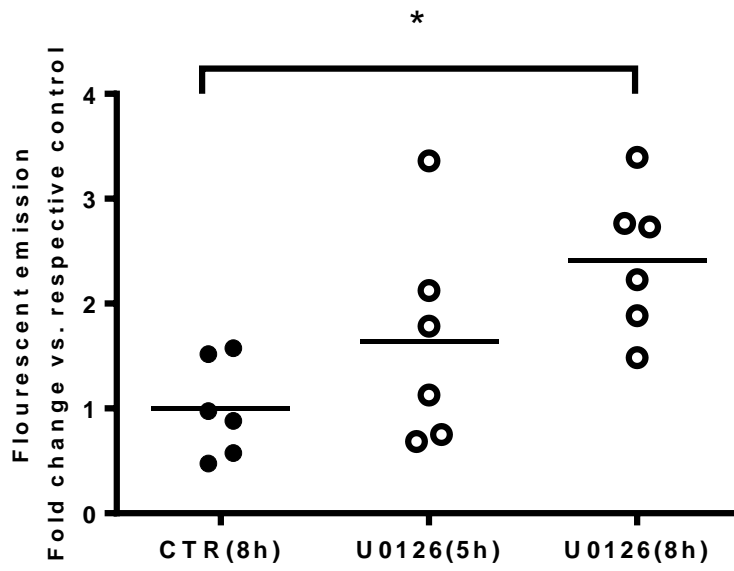
accumulation was significantly increased (2-3 fold) in the tumours of mice treated with 5-ALA plus U0126 when compare to those treated with 5-ALA and the vehicle control (DMSO) (Figure 8). These results demonstrate that treatment of a MEK inhibitor prior to 5-ALA exposure increases PpIX accumulation *in vivo* when the mammary tumours arise spontaneously.



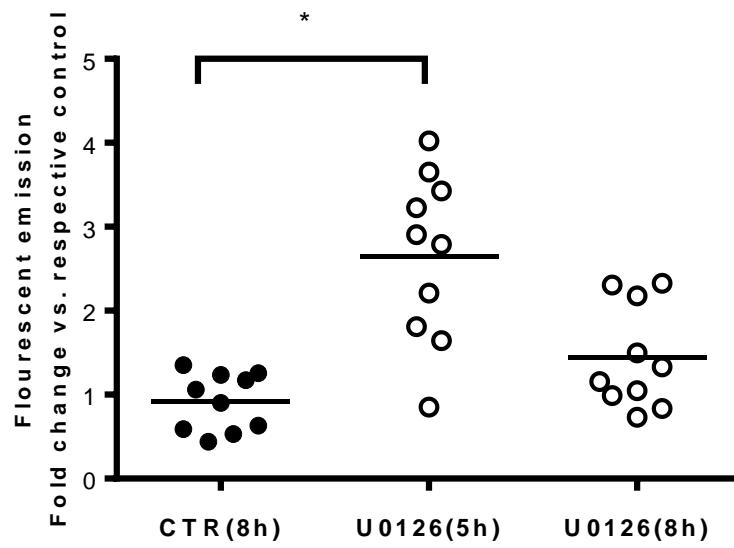
**Figure 8: Promotion of PpIX accumulation by MEK inhibition in 4T1 mammary tumour models**

Mouse breast cancer 4T1 cells were grown to 80% confluency and suspended in PBS. Subsequently,  $5 \times 10^5$  cells/100 $\mu$ l 4T1 cells were injected in the right hind flank of eight week old, female BALB/c mice. After the development of visible tumours (5-8 mm in diameter), the mice were injected it (A) or ip (B) with U0126 (50  $\mu$ M) for 5 or 8 h, or DMSO for 8 h, and ip with 5-ALA (200 mg/kg BW) for 2 h. Tumours were isolated for tissue homogenization and PpIX accumulation was determined by fluorescence microplate readings. (A: n = 6 mice per group; B: n = 10 mice per group)

A



B



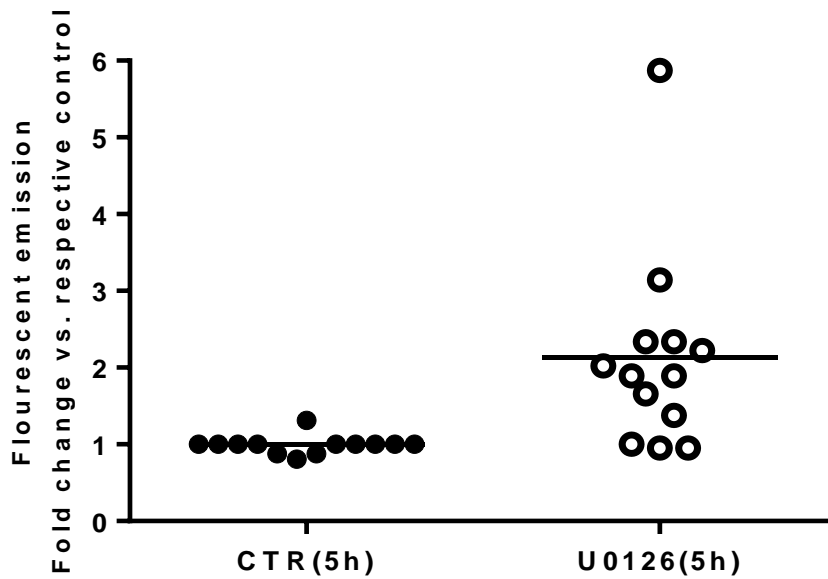


**Figure 9: Promotion of PpIX accumulation by MEK inhibition in H-Ras transgenic mice**

HRAS mice bearing mammary tumours at 3 months size range between 2-10 mm in diameter. Mice were injected ip with U0126 (50  $\mu$ M/kg in 100  $\mu$ l DMSO/PBS), or DMSO/PBS alone, 5 before sacrifice. All mice were administered a tail vein injection of 5-ALA solution to achieve a final dose of 200 mg/ kg BW (100  $\mu$ l saline) 1 h prior to sacrifice (n = 13 mice per group).

### 3.4.2 *In vivo* tumour imaging by PpIX fluorescence

In the clinical setting, PpIX fluorescence is used for surgical guidance to distinguish tumours from normal tissue. Having measured increased fluorescence in isolated tumour lysates with the combination of U0126 and 5-ALA, we examined whether treatment of the MEK inhibitor *in vivo* can enhance the fluorescence visibility of mammary tumours in mice. Balb/c mice bearing 4T1 tumours were injected IP with DMSO/saline for 5 h (Control), with DMSO/saline for 5 h plus 5-ALA for 2 h (5-ALA+DMSO) or with U0126 for 5 h and 5-ALA for 2 h (5-ALA+U0126) (Figure 9). PpIX fluorescence images were taken with Canon 6D digital camera with 35mm lens under blue light (380–440 nm). As shown in Figure 9, 5-ALA treatment induced PpIX fluorescence within the tumours while no PpIX fluorescence was observed in the tumours without 5-ALA injection (Control). Moreover, 5-ALA treatment combined with U0126 (5-ALA+U0126) showed enhanced PpIX fluorescence in the tumour compare to 5-ALA only treatment (5-ALA+DMSO). The combination treatment for the spontaneous HRAS transgenic mammary tumours was similarly imaged in untreated, 5-ALA treated or 5-ALA+U0126 treated animals. Like the 4T1 grafted tumour model, enhanced PpIX fluorescence was visible in the isolated tumours, both to the eye and the camera fitted with the emission filter (Figure 10). These results further demonstrate the practical value for *in vivo* promotion of PpIX fluorescence by MEK inhibition and the potential for improved tumour contrast during FGS.



**Figure 10: Real time visualization of PpIX accumulation by MEK inhibitor in 4T1 tumours**

Mammary 4T1 Tumour were illuminated with blue light (380–440 nm) generated by a D-light system (Storz GmbH, Tuttlingen, Germany) to excite PpIX fluorescence. Digital images were taken with a Canon 6D camera with 36 mm lens that was fitted with a yellow 635 nm emission filter.

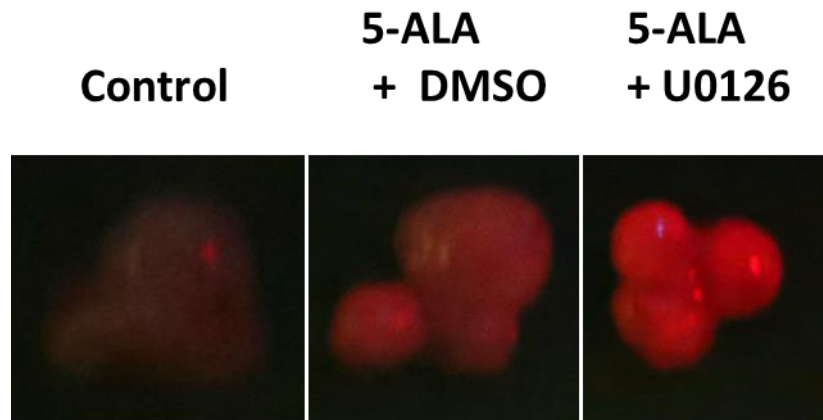


**Figure 11: Real time visualization of PpIX accumulation by MEK inhibitor in HRAS tumours**

HRAS mammarye tumour were illuminated with blue light (380–440 nm) generated by a D-light system (Storz GmbH, Tuttlingen, Germany) to excite PpIX fluorescence. Digital images were taken with a Canon 6D camera with 36 mm lens that was fitted with a yellow 635 nm emission filter.

## Chapter 4: Discussion

### 4.1 General Discussion

Fluorescence-guided resection of tumours is a novel approach for the surgical management of cancer patients. Although PpIX fluorescence is the most commonly used method for fluorescence-guided resection, insufficient PpIX accumulation often limits its benefit in certain types of tumours (Wang et al. 2013). Therefore, the objective of my research project was to determine if modulation of cell signalling pathways promotes PpIX accumulation induced by 5-ALA treatment in cancer cell lines and animal models of cancer.

The selection of the signalling pathway to target was influenced by a prior finding in Dr. Hirasawa's laboratory, where a novel interaction was noted between the heme biosynthesis and the oncogenic Ras/MEK pathways. In a cell culture model, it was found that pharmacological inhibition of MEK in transformed mouse fibroblast cells that have constitutively up-regulated RAS/MEK signalling activity led to promotion of PpIX accumulation induced by 5-ALA treatment (unpublished data). To validate this result, they examined human normal and cancer cells to determine whether PpIX accumulation can be promoted in human cell lines with the same drug combination. They concluded in this pilot experiment, that PpIX accumulation was promoted by MEK inhibition in human cancer cells but not in normal cells (unpublished data), which is a necessary requirement for FGS applications. To build on these promising results, my MSc project objectives were to determine: 1) whether MEK inhibition promotes PpIX

accumulation in different subtypes of cancer, and 2) whether MEK inhibition promotes PpIX accumulation in mouse models of breast cancer.

#### **4.2 *In vitro* experimental models**

To investigate the generalizability of PpIX promotion using the drug combination of 5-ALA plus the MEK inhibitor U0126, an expanded screening panel of human normal and cancer cells were selected, including breast, lung and prostate cancer cells. I found that MEK inhibition leads to enhanced PpIX accumulation in 4 of 6 breast cancer cell lines examined (Hs578-T, MDA MB 231, T47D, and MCF7), but not in BT474 and MDA MB 468 cells. Previous studies have examined a selection of this breast cancer cell line panel for PpIX accumulation in culture, including MCF7 and MDA MB 231. Similar to our study, these breast cancer cell lines showed enhanced PpIX fluorescence above the normal “immortalized” cell line MCF10A after 5-ALA treatment (Millon et al 2010). Our study is the first to show enhanced PpIX loading with the combination of 5-ALA and U0126 in breast cancer cell lines, which may have clinical value for FGS in breast cancer (Frei et al. 2004; Vahrmeijer et al. 2013; Ladner et al. 2001).

Enhanced PpIX accumulation was also observed in 3 of 4 lung cancer cell lines (A549, H460, H1299) but not in H1975 cell line. PpIX loading was also very high with 5-ALA alone in H1975, suggesting a limit to the potential for improvement with U0126 addition (data not shown). As per our findings, a previous study has reported PpIX accumulation by 5-ALA treatment in A549 lung cancer cells when treated with 5-ALA, but enhanced PpIX with the U0126



combination is a novel finding for the lung cancer cell lines we examined, which is very promising for FGS applications (Ali et al. 2011).

For prostate cancer, the results of our study showed 2 of 4 prostate cancer cell lines (DU145, LnCaP) with higher PpIX levels following treatment with 5-ALA and the U0126 MEK inhibitor, but no enhancement observed in PC-3 or 22Rv1 cell lines. One other study reported 5-ALA leads to PpIX enhancement in LNCaP cells for the purpose PDT treatment (Ortel et al. 2002). For those two cell lines that showed no PpIX enhancement, the expression of the Raf/MEK/ERK cascade is reported to be at lower activity levels, which may explain the lack of effect of the MEK inhibitor U0126 in these cell lines (McCubrey et al. 2007b). This concept could be important for any FGS-personalized medicine strategy, wherein culture models or human tumour biopsies are examined for biomarkers of the Raf/MEK/ERK activation state, as a predictor of PpIX fluorescence enhancement in the presence of 5-ALA. PpIX accumulation wasn't observed in the two cell lines originated from normal prostate tissues (Hs578-BST, MRC5), again confirming the specificity of PpIX loading for cancer cells, even in the presence of 5-ALA plus U0126. These overall results of the cell culture investigations suggest that MEK inhibition promotes PpIX accumulation in a broad range of cancer cells treated with 5-ALA.

### **4.3 *In vivo* experimental models**

After conducting *in vitro* experiments using different human cancer cell lines, we decided to determine whether PpIX accumulation can be similarly

promoted in mammary tumours that were grafted or developed spontaneously in mouse models. For the grafting experiments, we first screened three mouse mammary cancer cell lines for promotion of PpIX accumulation by MEK inhibition and found that promotion of PpIX accumulation by MEK inhibition was highest in mouse breast cancer 4T1 cells. Mice bearing 4T1 tumours inoculated on the hind flank were subsequently injected it or ip with U0126 and then PpIX accumulation in the tumours were measured at 5 and 8 h after injection, incorporating a 1 h incubation of an IP 5-ALA dose. We observed significant promotion of PpIX accumulation only at 8 h for it injection and at both 5 and 8 h for ip injection of U0126. In it injected-mice, we observed internal bleeding within the tumours caused by the U0126 injection. As contamination of red blood cells in the tumour lysates influences PpIX assay, this may be the reason that the promotion was not observed in mice it injected at the earlier time point (5 h).

In addition to the grafted model of mammary tumour cells, we examined whether treatment of MEK inhibitor promotes PpIX accumulation in a more heterogeneous population of tumour cells, as reflected by spontaneous mammary tumours arising in a transgenic mouse strain. Male mice of the HRAS transgenic line develop mammary adenosquamous carcinomas at approximately 3 months of age, under mammary epithelium driven expression of the Harvey rat sarcoma viral oncogene that integrated on Chr Y (Andres et al. 1987). This strain was examined in a previous study conducted by Dorward *et al* (2005), establishing significant PpIX accumulation selectively in tumour cells following 5-

ALA administration. In our study, *in vivo* MEK inhibition significantly increased PpIX fluorescence induced by 5-ALA treatment in the mammary tumours of the transgenic males. Our findings in both animals models were consistent, supporting enhanced PpIX accumulation with the combination of 5-ALA plus U0126, which is a very promising outcome for fluorescence improvements in FGS applications. Our *in vivo* studies warrant further animal and pre-clinical studies in the future, to r alternate MEK inhibitors and to further the exploration of the mechanism of PpIX enhancement suggested by cell culture models.

#### **4.4 Possible mechanisms of PpIX accumulation by U0126 MEK inhibitor**

MEK inhibition promoted PpIX accumulation in a cancer specific manner *in vitro* and *in vivo*. However, the molecular mechanisms of the promotion of PpIX accumulation still remain to be studied. Based on literature evidence predominantly determined in cell culture systems, there are three suggested mechanisms:

1. Downregulation of ATP-binding cassette (ABC) transporter family (ABCG2).
2. Downregulation of ferrochelatase (FECH) activity.
3. Reduction of cellular pH by MEK inhibition.

##### **4.4.1 Downregulation of ABCG2 by U0126**

ABCG2, a member of protein family of ATP-binding cassette (ABC) transporters, serves a cellular function to reduce PpIX accumulation in the

mitochondria by regulating its efflux to intracellular environment. Cancer cells frequently overexpress ABCG2 and it is notable that the expression level of ABCG2 is higher in cancer stem cells and drug-resistant cancer cells (Diestra et al. 2002; Jonker et al. 2002; Robey et al. 2005). The role of ABCG2 as a chemical transporter is to limit the absorption or re-uptake of drugs and toxins in our diet and to maintain intact cellular homeostasis by efflux out potentially toxic chemicals or chemotherapeutic drugs. The first study to prove this mechanism showed that oral bioavailability of topotecan (Chemotherapy agent) was significantly increased in mice treated with an ABCG2 inhibitor (Allen et al. 1999). Therefore, ABCG2 is recognized as a biomarker for predicting drug resistance cancer cells (Bessho et al. 2006).

One of the possible mechanisms for promotion of PpIX accumulation by MEK inhibition is downregulation of ABCG2 transporter protein expression. Imai et al. (2009) reported for human MCF-7 breast cancer cells and NCI-N87 colon cancer cells treated with the MEK inhibitor U0126, there was increased degradation of the ABCG2 transporter protein leading to increased net accumulation of anticancer agents. Another study demonstrated that a MAPK inhibitor led to degradation of ABCG2 protein, therefore suggesting that MAPK pathway inhibition is a strategy for overcoming ABCG2-mediated multidrug resistance in laryngeal squamous cell carcinoma (Xie et al. 2014). These studies both support the ABCG2 transporter as a downstream expression target of the MEK pathway that is sensitive to signalling pathway activity. Furthermore,

overexpression studies implicate the ABCG2 transporter as a primary controller of PpIX accumulation. In colon cancer cells (SW480), engineered overexpression of ABCG2 reduced 5-ALA induced PpIX fluorescence, both *in vitro* and *in vivo* (Kim et al. 2015). Similarly, inhibitors of ABCG2 transporter, such as Ko143 (Asashima et al. 2006) and Elacridar were reported to increase PpIX accumulation in cells treated with 5-ALA, as part of a study to examine the role of human ABC transporter ABCG2 in photodynamic diagnosis (PDD)(Ishikawa et al. 2011). These results indicate that PpIX loading is dependent on ABCG2 expression level. Therefore, downregulation of ABCG2 transporter may be one of the mechanisms that underlies the promotion of PpIX accumulation with MEK inhibition. ABCG2 inhibitors have received significant attention for the development of chemical inhibitors to overcome drug resistance in cancer patients; however, the inhibition of ABCG2 transport with these inhibitors is not cancer-cell specific, thus undermining the potential benefit of ABCG2 inhibitor to increase cancer-specific PpIX loading (To and Tomlinson 2013).

#### **4.4.2 Downregulation or inhibition of FECH by U0126**

Another possible mechanism by which MEK inhibition could influence PpIX accumulation is to influence the enzyme expression and activity of the heme synthesis pathway. The heme biosynthetic pathway consists of several enzymatic steps (Figure 2). FECH, the terminal enzyme of the pathway, converts PpIX into non-fluorescent heme with the incorporation of the iron atom, as one of the rate limiting steps for heme synthesis (Olsson et al. 2002). Downregulation of

FECH expression is considered to play a major role in the intracellular PpIX accumulation (Kemmner et al. 2008). Moreover, low expression of FECH in malignant tumours, such as colon cancer and urothelial cancer, is correlated with high intracellular PpIX accumulation in tumour cells (Peng et al. 1997). Inhibition of FECH by iron chelator deferoxamine (DFX) and NOC-18 through nitric generation have been reported to promote cellular PpIX accumulation in 5-ALA-treated human oral squamous cell carcinoma HSC-4 cells (Yamamoto et al. 2013). In another study, significant accumulation of PpIX was also observed by inhibition of FECH using deferoxamine and NOC-18 in ALA-treated prostate cancer PC-3 cells (Fukuhara et al. 2013). Furthermore, silencing FECH by siRNA promotes PpIX accumulation in human glioma cell lines SNB19 and U87 (Kemmner et al. 2008). Finally, the injection of dendritic nanocarriers containing FECH siRNA promoted the fluorescence detection of tumours in an animal tumour model (Wan et al. 2012). However, there has been no report that indicates regulation of FECH activity is influenced by MEK activity. Nevertheless, it is still possible that MEK inhibition promotes PpIX accumulation by down-regulating FECH.

#### **4.4.3 Reduction of cellular pH by MEK inhibition**

Several studies have reported that the tumour's microenvironment may lead to PpIX accumulation after 5-ALA administration. In general, pH is lower in the tumour external environment compared to normal tissue (Gerweck and Seetharaman 1996). Certain enzymes in the heme biosynthesis pathway function

optimally at lower pH. For instance, PBG-D at a pH of 6.2-6.4 forms the skeletal structure of porphyrinogen (Balgi et al. 2011). A different research group showed the enhancement of PpIX after 5-ALA administration by lowering tumour pH with Glucose (Piot et al. 2001). In addition, inhibition of RAF-ERK-MEK pathway leads to acidic environment in tumour cells. One study showed that inhibition of ERK-activating Thr<sup>202</sup>/Tyr<sup>204</sup> phosphorylation by PD98059 in human breast cancer MCF-7 cells leads to an extracellular acidic environment of pH 6.2 (Balgi et al. 2011) which may represent another possibility of PpIX accumulation by U0126. If an acidic environment leads to increased PpIX accumulation, inhibition of RAF-ERK-MEK by U0126 may promote PpIX accumulation indirectly. According to these studies combination of outcomes by MEK inhibition could enhance PpIX accumulation. All the mechanisms described are not mutually exclusive.

#### **4.5 Compounds that leads to PpIX accumulation**

There are other compounds that are known to promote PpIX accumulation *in vitro*. Here, I will discuss about them in comparison with MEK inhibitors.

##### **4.5.1 ABCG2 inhibitors**

ABCG2 is widely expressed in both normal and cancer cells (G. Zhang et al. 2013). According to previous studies, ABCG2 inhibitors lead to PpIX accumulation in short time (60 m) in cancer cells (Asashima et al. 2006) compare to MEK inhibitors (10-20 h). However, Hirasawa lab observed that ABCG2

inhibitors promote PpIX accumulation in normal cells (Ema Yoshioka 2015). Therefore, the advantage to use MEK inhibitors over ABCG2 inhibitors in the clinical settings is their cancer specificity. This is very important because by accumulation of PpIX in normal cells surgeon is unable to distinguish normal cells from cancer cells.

#### **4.5.2 FECH inhibitors**

FECH plays a major role in the final step of heme synthesis as it converts protoporphyrin IX (PpIX) to functional heme. Inhibition of FECH leads to increase PpIX accumulation. However, increase PpIX levels by FECH inhibition alone is often not sufficient to increase PpIX accumulation (Yamamoto et al. 2013). FECH inhibitors are required to be treated with other compounds to have significant effect on the PpIX accumulation. Therefore, MEK inhibitors may be an ideal candidate for the combined treatment.

#### **4.5.3 Feasibility of MEK inhibitors for use in FGS applications**

The MAPK pathway is one of the most deregulated signal transduction pathways in human cancer. Several MEK inhibitors have been developed and evaluated in different clinical studies. One of the MEK inhibitors, Trametinib, has been approved for clinical use by the FDA (National Cancer Institute 2016). In general, MEK inhibitors are well tolerated in the clinical setting with the most common side effects being minor, such as diarrhoea, rash and fatigue. Given that both MEK inhibitors and 5-ALA are already approved for clinical use, the combination of a MEK inhibitor and 5-ALA to enhance PpIX in cancer cells would



be a feasible idea for FGS applications. There are several possible advantages from this drug combination, in addition to improved FGS sensitivity: 1) MEK inhibitors have independent antitumour effects and could, therefore, act additively or synergistically with anti-cancer effects when patients are treated with PDT or chemotherapy; 2) potential reduction of 5-ALA dosing to reduce the side effects of peripheral nerve pain and burning sensations when patients treated with 5-ALA are exposed to light; (Kemmner et al. 2008). 3) MEK inhibitors have the potential to enhance the efficiency of chemotherapeutic drugs by inhibiting the efflux of the drug out of the cell through an ABCG2-directed mechanism.

#### **4.6 Conclusion**

1) The promotion of PpIX accumulation by MEK inhibition enhanced PpIX accumulation in certain cancer cell models (breast, lung, prostate) in this study. On the other hand, there were cancer cell lines in which PpIX accumulation was not observed along with two normal immortal cell lines. It is important to investigate the molecular mechanism of PpIX accumulation to overcome the resistant cellular population. This study shows the cancer specificity of PpIX accumulation by MEK inhibitor which is very important in FGS to distinguish normal tissue from tumours.

2) The MEK inhibitor demonstrated its ability to promote PpIX accumulation in *in vivo* cancer models Based on the results, I believe that MEK inhibitors

have a great potential to improve visualization of tumour fluorescence, which support the tumour resection in the clinical settings.

#### 4.7 Future Directions

- 1) Identification of which molecule of the heme biosynthesis pathway is regulated by Ras/MEK.

The heme biosynthesis pathway is regulated by several enzymes such as delta aminolevulinic acid synthase (ALAS), ALA dehydratase (ALAD), porphobilinogen deaminase (PBGD), uroporphyrinogen-III synthase (UROS), uroporphyrinogen decarboxylase (UROD), prophyrinogen oxidase (CPO) and protoporphyrinogen oxidase (PPO) (Figure 2). Activation of these enzymes promotes accumulation of PpIX. In contrast, ferrochelatase (FECH)-mediated insertion of iron into PpIX and ATP-binding cassette sub-family G-2(ABCG2) transport activity both reduce the fluorescent PpIX pool within the cell. FECH activity can be measured using the method described by van Hillegeresberg in absence or presence of a MEK inhibitor (Kemmner et al. 2008).

Furthermore, the expression levels of these enzymes can be determined in human cancer cells treated with or without U0126 by Western blot analysis and qRT-PCR.

- 2) Determine whether the MEK inhibitors are effective to enhance visualization of metastatic foci in animal models.

FGS can be used to remove metastatic foci in clinical settings. I believe that combined treatment of 5-ALA with MEK inhibitor would improve the detection

of metastatic foci. To determine this, metastatic mouse cancer models will be established by iv injection of a metastatic cancer cells line. Mice will be treated ip with 5-ALA and with Selumetinib (50/100  $\mu$ M). The visualization of metastatic foci will be evaluated by whole body imaging analysis. The lungs will be removed and tumour fragments isolated for tissue homogenization to determine PpIX accumulation by microplate fluorescence readings.

- 3) Determine whether combination of the MEK inhibitor and 5-ALA leads to more effective FGS of brain tumours.

High grade gliomas are extremely aggressive and, despite of different options for treatment, the prognosis is poor. Although complete resection of malignant glioma is essential for patient's survival, it is difficult to be achieved as the margins between tumours and normal tissues are unclear. Therefore, gliomas are the type of cancers where a significant improvement of FGS techniques are needed most. Therefore, it is critical to determine whether MEK inhibitor could improve tumour visualization in mouse glioma models. Mice implanted with glioma tumours will be treated ip with 5-ALA and with Selumetinib (50/100  $\mu$ M). The visualization of the brain will be evaluated by live imaging analysis to determine PpIX accumulation.

## Bibliography

- Ali, Abdellah Hamed Khalil, Hiromitsu Takizawa, Kazuya Kondo, Hisashi Matsuoka, Hiroaki Toba, Yasushi Nakagawa, Koichiro Kenzaki, et al. 2011. "5-Aminolevulinic Acid-Induced Fluorescence Diagnosis of Pleural Malignant Tumor." *Lung Cancer* 74 (1): 48–54. doi:10.1016/j.lungcan.2011.01.031.
- Allen, J D, R F Brinkhuis, J Wijnholds, and A H Schinkel. 1999. "The Mouse Bcrp1/Mxr/Abcp Gene: Amplification and Overexpression in Cell Lines Selected for Resistance to Topotecan, Mitoxantrone, or Doxorubicin." *Cancer Research* 59 (17): 4237–41. <http://www.ncbi.nlm.nih.gov/pubmed/10485464>.
- Allison, Ron R. 2015. "Fluorescence Guided Resection (FGR): A Primer for Oncology." *Photodiagnosis and Photodynamic Therapy* 13 (November). Elsevier: 73–80. doi:10.1016/j.pdpdt.2015.11.008.
- Andres, A C, C A Schönenberger, B Groner, L Hennighausen, M LeMeur, and P Gerlinger. 1987. "Ha-Ras Oncogene Expression Directed by a Milk Protein Gene Promoter: Tissue Specificity, Hormonal Regulation, and Tumor Induction in Transgenic Mice." *Proceedings of the National Academy of Sciences of the United States of America* 84 (5): 1299–1303. <http://www.pubmedcentral.nih.gov/articlerender.fcgi?artid=304415&tool=pmc-entrez&rendertype=abstract>.
- Asashima, Tomoko, Satoko Hori, Sumio Ohtsuki, Masanori Tachikawa, Masahiko Watanabe, Chisato Mukai, Shinji Kitagaki, Naoki Miyakoshi, and Tetsuya Terasaki. 2006. "ATP-Binding Cassette Transporter G2 Mediates the Efflux of Phototoxins on the Luminal Membrane of Retinal Capillary Endothelial Cells." *Pharmaceutical Research* 23 (6): 1235–42. doi:10.1007/s11095-006-0067-2.
- Balgi, Aruna D, Graham H Diering, Elizabeth Donohue, Karen K Y Lam, Bruno D Fonseca, Carla Zimmerman, Masayuki Numata, and Michel Roberge. 2011.

- “Regulation of mTORC1 Signaling by pH.” *PloS One* 6 (6). Public Library of Science: e21549. doi:10.1371/journal.pone.0021549.
- Banks-Schlegel, S P, A F Gazdar, and C C Harris. 1985. “Intermediate Filament and Cross-Linked Envelope Expression in Human Lung Tumor Cell Lines.” *Cancer Research* 45 (3): 1187–97.  
<http://www.ncbi.nlm.nih.gov/pubmed/2578876>.
- Bertram, J S, and P Janik. 1980. “Establishment of a Cloned Line of Lewis Lung Carcinoma Cells Adapted to Cell Culture.” *Cancer Letters* 11 (1): 63–73.  
<http://www.ncbi.nlm.nih.gov/pubmed/7226139>.
- Bessho, Yuji, Tetsuya Oguri, Hiroyuki Achiwa, Hideki Muramatsu, Hiroyoshi Maeda, Takashi Niimi, Shigeki Sato, and Ryuzo Ueda. 2006. “Role of ABCG2 as a Biomarker for Predicting Resistance to CPT-11/SN-38 in Lung Cancer.” *Cancer Science* 97 (3): 192–98. doi:10.1111/j.1349-7006.2006.00164.x.
- Blinman, Prunella, Corona Gainford, Mark Donoghoe, Julie Martyn, Penny Blomfield, Peter Grant, Ganessan Kichenadasse, et al. 2013. “Feasibility, Acceptability and Preferences for Intraperitoneal Chemotherapy with Paclitaxel and Cisplatin after Optimal Debulking Surgery for Ovarian and Related Cancers: An ANZGOG Study.” *Journal of Gynecologic Oncology* 24 (4): 359–66. doi:10.3802/jgo.2013.24.4.359.
- Bodai, Balazs I, and Phillip Tusó. 2015. “Breast Cancer Survivorship: A Comprehensive Review of Long-Term Medical Issues and Lifestyle Recommendations.” *The Permanente Journal* 19 (2). Kaiser Permanente: 48–79. doi:10.7812/TPP/14-241.
- Borisova, Ekaterina, Lilia Plamenova, Momchil Keremedchiev, Borislav Vladimirov, and Latchezar Avramov. 2013. “Endogenous and Exogenous Fluorescence of Gastrointestinal Tumors: Initial Clinical Observations.” In *Seventeenth International School on Quantum Electronics: Laser Physics*

*and Applications*, edited by Tanja N. Dreischuh and Albena T. Daskalova, 87701C. International Society for Optics and Photonics.  
doi:10.1117/12.2016389.

Brinkley, B R, P T Beall, L J Wible, M L Mace, D S Turner, and R M Cailleau. 1980. "Variations in Cell Form and Cytoskeleton in Human Breast Carcinoma Cells in Vitro." *Cancer Research* 40 (9): 3118–29.  
<http://www.ncbi.nlm.nih.gov/pubmed/7000337>.

Bung, Navneet, Meenakshi Pradhan, Harini Srinivasan, and Gopalakrishnan Bulusu. 2014. "Structural Insights into E. Coli Porphobilinogen Deaminase during Synthesis and Exit of 1-Hydroxymethylbilane." *PLoS Computational Biology* 10 (3): e1003484. doi:10.1371/journal.pcbi.1003484.

Burke, Siún, and George D Shorten. 2009. "When Pain after Surgery Doesn't Go Away..." *Biochemical Society Transactions* 37 (Pt 1): 318–22.  
doi:10.1042/BST0370318.

"Canadian Cancer Statistics." 2015. *Canadian Cancer Society*.  
<http://www.cancer.ca/en/cancer-information/cancer-101/cancer-statistics-at-a-glance/?region=nl>.

Cargnello, Marie, and Philippe P Roux. 2011. "Activation and Function of the MAPKs and Their Substrates, the MAPK-Activated Protein Kinases." *Microbiology and Molecular Biology Reviews : MMBR* 75 (1): 50–83.  
doi:10.1128/MMBR.00031-10.

Chakraborty, Arup R, Robert W Robey, Victoria L Luchenko, Zhirong Zhan, Richard L Piekarz, Jean-Pierre Gillet, Andrew V Kossenkov, et al. 2013. "MAPK Pathway Activation Leads to Bim Loss and Histone Deacetylase Inhibitor Resistance: Rationale to Combine Romidepsin with an MEK Inhibitor." *Blood* 121 (20): 4115–25. doi:10.1182/blood-2012-08-449140.

Collaud, Sabine, Asta Juzeniene, Johan Moan, and Norbert Lange. 2004. "On

- the Selectivity of 5-Aminolevulinic Acid-Induced Protoporphyrin IX Formation." *Current Medicinal Chemistry. Anti-Cancer Agents* 4 (3): 301–16. <http://www.ncbi.nlm.nih.gov/pubmed/15134506>.
- de Visscher, S A H J, P U Dijkstra, I B Tan, J L N Roodenburg, and M J H Witjes. 2013. "mTHPC Mediated Photodynamic Therapy (PDT) of Squamous Cell Carcinoma in the Head and Neck: A Systematic Review." *Oral Oncology* 49 (3): 192–210. doi:10.1016/j.oraloncology.2012.09.011.
- Dhillon, A S, S Hagan, O Rath, and W Kolch. 2007. "MAP Kinase Signalling Pathways in Cancer." *Oncogene* 26 (22): 3279–90. doi:10.1038/sj.onc.1210421.
- Diestra, Julio E, George L Scheffer, Isabel Català, Marc Maliepaard, Jan H M Schellens, Rik J Scheper, Jose R Germà-Lluch, and Miguel A Izquierdo. 2002. "Frequent Expression of the Multi-Drug Resistance-Associated Protein BCRP/MXR/ABCP/ABCG2 in Human Tumours Detected by the BXP-21 Monoclonal Antibody in Paraffin-Embedded Material." *The Journal of Pathology* 198 (2): 213–19. doi:10.1002/path.1203.
- Dorward, A M, K S Fancher, T M Duffy, W G Beamer, and H Walt. 2005. "Early Neoplastic and Metastatic Mammary Tumours of Transgenic Mice Detected by 5-Aminolevulinic Acid-Stimulated Protoporphyrin IX Accumulation." *British Journal of Cancer* 93 (10): 1137–43. doi:10.1038/sj.bjc.6602840.
- Duncia, J V, J B Santella, C A Higley, W J Pitts, J Wityak, W E Fietze, F W Rankin, et al. 1998. "MEK Inhibitors: The Chemistry and Biological Activity of U0126, Its Analogs, and Cyclization Products." *Bioorganic & Medicinal Chemistry Letters* 8 (20): 2839–44. <http://www.ncbi.nlm.nih.gov/pubmed/9873633>.
- Ema Yoshioka, Ken Hirasawa. 2015. "An Unexpected Branching-out from Viral Oncolysis to PpIX Research." In *Toronto Univeristy*. TORONTO.

- Ema Yoshioka, Ken Hirasawa, Ann Dorward. 2014. "Promotion of Protoporphyrin IX (PpIX) Fluorescence by MEK Inhibition in in Vivo Cancer Models." In *BHCRI/TFRI Cancer Research*. Halifax.
- "FDA Approval for Trametinib - National Cancer Institute." 2016. Accessed April 16. <http://www.cancer.gov/about-cancer/treatment/drugs/fda-trametinib>.
- Frankel, Timothy L, Jennifer LaFemina, Zubin M Bamboat, Michael I D'Angelica, Ronald P DeMatteo, Yuman Fong, T Peter Kingham, William R Jarnagin, and Peter J Allen. 2013. "Dysplasia at the Surgical Margin Is Associated with Recurrence after Resection of Non-Invasive Intraductal Papillary Mucinous Neoplasms." *HPB: The Official Journal of the International Hepato Pancreato Biliary Association* 15 (10): 814–21. doi:10.1111/hpb.12137.
- Frei, K A, H M Bonel, H Frick, H Walt, and R A Steiner. 2004. "Photodynamic Detection of Diseased Axillary Sentinel Lymph Node after Oral Application of Aminolevulinic Acid in Patients with Breast Cancer." *British Journal of Cancer* 90 (4): 805–9. doi:10.1038/sj.bjc.6601615.
- Fujita, Hirofumi, Keisuke Nagakawa, Hirotsugu Kobuchi, Tetsuya Ogino, Yoichi Kondo, Keiji Inoue, Taro Shuin, et al. 2016. "Phytoestrogen Suppresses Efflux of the Diagnostic Marker Protoporphyrin IX (PpIX) in Lung Carcinoma." *Cancer Research*, February. doi:10.1158/0008-5472.CAN-15-1484.
- Fukuhara, Hideo, Keiji Inoue, Atsushi Kurabayashi, Mutsuo Furihata, Hirofumi Fujita, Kozo Utsumi, Junzo Sasaki, and Taro Shuin. 2013. "The Inhibition of Ferrochelatase Enhances 5-Aminolevulinic Acid-Based Photodynamic Action for Prostate Cancer." *Photodiagnosis and Photodynamic Therapy* 10 (4): 399–409. doi:10.1016/j.pdpdt.2013.03.003.
- Gamelin, Erick, Remy Delva, Jacques Jacob, Yacine Merrouche, Jean Luc Raoul, Denis Pezet, Etienne Dorval, Gilles Piot, Alain Morel, and Michele Boisdron-Celle. 2008. "Individual Fluorouracil Dose Adjustment Based on



- Pharmacokinetic Follow-up Compared with Conventional Dosage: Results of a Multicenter Randomized Trial of Patients with Metastatic Colorectal Cancer." *Journal of Clinical Oncology : Official Journal of the American Society of Clinical Oncology* 26 (13): 2099–2105.  
doi:10.1200/JCO.2007.13.3934.
- Gerber, David E. 2008. "Targeted Therapies: A New Generation of Cancer Treatments." *American Family Physician* 77 (3): 311–19.  
<http://www.ncbi.nlm.nih.gov/pubmed/18297955>.
- Gerweck, Leo E., and Kala Seetharaman. 1996. "Cellular pH Gradient in Tumor versus Normal Tissue: Potential Exploitation for the Treatment of Cancer." *Cancer Res.* 56 (6): 1194–98.  
<http://cancerres.aacrjournals.org/content/56/6/1194>.
- Giaccone, G, J Battey, A F Gazdar, H Oie, M Draoui, and T W Moody. 1992. "Neuromedin B Is Present in Lung Cancer Cell Lines." *Cancer Research* 52 (9 Suppl): 2732s – 2736s. <http://www.ncbi.nlm.nih.gov/pubmed/1563005>.
- Giard, D J, S A Aaronson, G J Todaro, P Arnstein, J H Kersey, H Dosik, and W P Parks. 1973. "In Vitro Cultivation of Human Tumors: Establishment of Cell Lines Derived from a Series of Solid Tumors." *Journal of the National Cancer Institute* 51 (5): 1417–23. <http://www.ncbi.nlm.nih.gov/pubmed/4357758>.
- Gibas, Z, R Becher, E Kawinski, J Horoszewicz, and A A Sandberg. 1984. "A High-Resolution Study of Chromosome Changes in a Human Prostatic Carcinoma Cell Line (LNCaP)." *Cancer Genetics and Cytogenetics* 11 (4): 399–404. <http://www.ncbi.nlm.nih.gov/pubmed/6584201>.
- Gioux, Sylvain, Hak Soo Choi, and John V Frangioni. 2010. "Image-Guided Surgery Using Invisible near-Infrared Light: Fundamentals of Clinical Translation." *Molecular Imaging* 9 (5): 237–55.  
<http://www.pubmedcentral.nih.gov/articlerender.fcgi?artid=3105445&tool=pmcentrez&rendertype=abstract>.

- Gottesman, Michael M, Tito Fojo, and Susan E Bates. 2002. "Multidrug Resistance in Cancer: Role of ATP-Dependent Transporters." *Nature Reviews. Cancer* 2 (1): 48–58. doi:10.1038/nrc706.
- Hackett, A J, H S Smith, E L Springer, R B Owens, W A Nelson-Rees, J L Riggs, and M B Gardner. 1977. "Two Syngeneic Cell Lines from Human Breast Tissue: The Aneuploid Mammary Epithelial (Hs578T) and the Diploid Myoepithelial (Hs578Bst) Cell Lines." *Journal of the National Cancer Institute* 58 (6): 1795–1806. <http://www.ncbi.nlm.nih.gov/pubmed/864756>.
- Hawkins, Thomas A, Florencia Cavodeassi, Ferenc Erdélyi, Gábor Szabó, and Zsolt Lele. 2008. "The Small Molecule Mek1/2 Inhibitor U0126 Disrupts the Chordamesoderm to Notochord Transition in Zebrafish." *BMC Developmental Biology* 8 (January): 42. doi:10.1186/1471-213X-8-42.
- Hirche, Christoph, Dawid Murawa, Zarah Mohr, Soeren Kneif, and Michael Hünerbein. 2010. "ICG Fluorescence-Guided Sentinel Node Biopsy for Axillary Nodal Staging in Breast Cancer." *Breast Cancer Research and Treatment* 121 (2): 373–78. doi:10.1007/s10549-010-0760-z.
- Hoffmann, Katrin, Lin Shibo, Zhi Xiao, Thomas Longerich, Markus W Büchler, and Peter Schemmer. 2011. "Correlation of Gene Expression of ATP-Binding Cassette Protein and Tyrosine Kinase Signaling Pathway in Patients with Hepatocellular Carcinoma." *Anticancer Research* 31 (11): 3883–90. <http://www.ncbi.nlm.nih.gov/pubmed/22110214>.
- Huang, Z. 2005. "A Review of Progress in Clinical Photodynamic Therapy." *Technology in Cancer Research & Treatment* 4 (3): 283–93. <http://www.pubmedcentral.nih.gov/articlerender.fcgi?artid=1317568&tool=pmcentrez&rendertype=abstract>.
- Imai, Yasuo, Kyoko Ohmori, Shin'ichi Yasuda, Mariko Wada, Tsukasa Suzuki, Kazunori Fukuda, and Yoshihiko Ueda. 2009. "Breast Cancer Resistance protein/ABCG2 Is Differentially Regulated Downstream of Extracellular

Signal-Regulated Kinase.” *Cancer Science* 100 (6): 1118–27.

doi:10.1111/j.1349-7006.2009.01154.x.

Inoue, Keiji, Hideyasu Matsuyama, Kiyohide Fujimoto, Yoshihiko Hirao, Hironobu Watanabe, Seiichiro Ozono, Masafumi Oyama, et al. 2016. “The Clinical Trial on the Safety and Effectiveness of the Photodynamic Diagnosis of Non-Muscle-Invasive Bladder Cancer Using Fluorescent Light-Guided Cystoscopy after Oral Administration of 5-Aminolevulinic Acid (5-ALA).” *Photodiagnosis and Photodynamic Therapy*, January.  
doi:10.1016/j.pdpdt.2015.12.011.

Ishikawa, Toshihisa, Kenkichi Takahashi, Naokado Ikeda, Yoshinaga Kajimoto, Yuichiro Hagiya, Shun-Ichiro Ogura, Shin-Ichi Miyatake, and Toshihiko Kuroiwa. 2011. “Transporter-Mediated Drug Interaction Strategy for 5-Aminolevulinic Acid (ALA)-Based Photodynamic Diagnosis of Malignant Brain Tumor: Molecular Design of ABCG2 Inhibitors.” *Pharmaceutics* 3 (3): 615–35. doi:10.3390/pharmaceutics3030615.

Jacobs, J P, C M Jones, and J P Baille. 1970. “Characteristics of a Human Diploid Cell Designated MRC-5.” *Nature* 227 (5254): 168–70.  
<http://www.ncbi.nlm.nih.gov/pubmed/4316953>.

Jonker, Johan W, Marije Buitelaar, Els Wagenaar, Martin A Van Der Valk, George L Scheffer, Rik J Scheper, Torsten Plosch, et al. 2002. “The Breast Cancer Resistance Protein Protects against a Major Chlorophyll-Derived Dietary Phototoxin and Protoporphyrin.” *Proceedings of the National Academy of Sciences of the United States of America* 99 (24): 15649–54.  
doi:10.1073/pnas.202607599.

Judge, S M, and R T Chatterton. 1983. “Progesterone-Specific Stimulation of Triglyceride Biosynthesis in a Breast Cancer Cell Line (T-47D).” *Cancer Research* 43 (9): 4407–12. <http://www.ncbi.nlm.nih.gov/pubmed/6871874>.

Kaighn, M E, K S Narayan, Y Ohnuki, J F Lechner, and L W Jones. 1979.

“Establishment and Characterization of a Human Prostatic Carcinoma Cell Line (PC-3).” *Investigative Urology* 17 (1): 16–23.  
<http://www.ncbi.nlm.nih.gov/pubmed/447482>.

Kemmner, Wolfgang, Kayiu Wan, Steffen Rüttinger, Bernd Ebert, Rainer Macdonald, Ursula Klamm, and K Thomas Moesta. 2008. “Silencing of Human Ferrochelatase Causes Abundant Protoporphyrin-IX Accumulation in Colon Cancer.” *FASEB Journal: Official Publication of the Federation of American Societies for Experimental Biology* 22 (2): 500–509.  
doi:10.1096/fj.07-8888com.

Kim, Ju Hee, Jae Myung Park, Yoon Jin Roh, In-Wook Kim, Tayyaba Hasan, and Myung-Gyu Choi. 2015. “Enhanced Efficacy of Photodynamic Therapy by Inhibiting ABCG2 in Colon Cancers.” *BMC Cancer* 15 (January): 504.  
doi:10.1186/s12885-015-1514-4.

Kobuchi, Hirotugu, Koko Moriya, Tetsuya Ogino, Hirofumi Fujita, Keiji Inoue, Taro Shuin, Tatsuji Yasuda, Kozo Utsumi, and Toshihiko Utsumi. 2012. “Mitochondrial Localization of ABC Transporter ABCG2 and Its Function in 5-Aminolevulinic Acid-Mediated Protoporphyrin IX Accumulation.” *PLoS ONE* 7 (11). doi:10.1371/journal.pone.0050082.

Kraft, John C, and Rodney J Y Ho. 2014. “Interactions of Indocyanine Green and Lipid in Enhancing near-Infrared Fluorescence Properties: The Basis for near-Infrared Imaging in Vivo.” *Biochemistry* 53 (8): 1275–83.  
doi:10.1021/bi500021j.

Ladner, D P, R A Steiner, J Allemann, U Haller, and H Walt. 2001. “Photodynamic Diagnosis of Breast Tumours after Oral Application of Aminolevulinic Acid.” *British Journal of Cancer* 84 (1): 33–37.  
doi:10.1054/bjoc.2000.1532.

Lakowicz, Joseph R. 2006. *Principles of Fluorescence Spectroscopy Principles of Fluorescence Spectroscopy*. doi:10.1007/978-0-387-46312-4.

- Lasfargues, E Y, W G Coutinho, and E S Redfield. 1978. "Isolation of Two Human Tumor Epithelial Cell Lines from Solid Breast Carcinomas." *Journal of the National Cancer Institute* 61 (4): 967–78.  
<http://www.ncbi.nlm.nih.gov/pubmed/212572>.
- Lau, Darryl, Shawn L Hervey-Jumper, Susan Chang, Annette M Molinaro, Michael W McDermott, Joanna J Phillips, and Mitchel S Berger. 2015. "A Prospective Phase II Clinical Trial of 5-Aminolevulinic Acid to Assess the Correlation of Intraoperative Fluorescence Intensity and Degree of Histologic Cellularity during Resection of High-Grade Gliomas." *Journal of Neurosurgery*, November, 1–10. doi:10.3171/2015.5.JNS1577.
- Lin, W C, S A Toms, M Johnson, E D Jansen, and A Mahadevan-Jansen. 2001. "In Vivo Brain Tumor Demarcation Using Optical Spectroscopy." *Photochemistry and Photobiology* 73 (4): 396–402.  
<http://www.ncbi.nlm.nih.gov/pubmed/11332035>.
- Loh, C S, A J MacRobert, J Bedwell, J Regula, N Krasner, and S G Bown. 1993. "Oral versus Intravenous Administration of 5-Aminolaevulinic Acid for Photodynamic Therapy." *British Journal of Cancer* 68 (1): 41–51.  
<http://www.pubmedcentral.nih.gov/articlerender.fcgi?artid=1968297&tool=pmcentrez&rendertype=abstract>.
- Maniar, A C, T W Williams, G W Hammond, N Johnson, and N L Kobrinsky. 1991. "Excretion of Mutagens Following Chemotherapy." *The American Journal of Pediatric Hematology/oncology* 13 (2): 160–63.  
<http://www.ncbi.nlm.nih.gov/pubmed/2069224>.
- Marcu, Laura, Javier A Jo, Pramod V Butte, William H Yong, Brian K Pikul, Keith L Black, and Reid C Thompson. "Fluorescence Lifetime Spectroscopy of Glioblastoma Multiforme." *Photochemistry and Photobiology* 80 (January): 98–103. doi:10.1562/2003-12-09-RA-023.1.
- Matsui, Aya, Eiichi Tanaka, Hak Soo Choi, Joshua H Winer, Vida Kianzad,

- Sylvain Gioux, Rita G Laurence, and John V Frangioni. 2010. "Real-Time Intra-Operative near-Infrared Fluorescence Identification of the Extrahepatic Bile Ducts Using Clinically Available Contrast Agents." *Surgery* 148 (1): 87–95. doi:10.1016/j.surg.2009.12.004.
- McCubrey, James A, Linda S Steelman, William H Chappell, Stephen L Abrams, Ellis W T Wong, Fumin Chang, Brian Lehmann, et al. 2007a. "Roles of the Raf/MEK/ERK Pathway in Cell Growth, Malignant Transformation and Drug Resistance." *Biochimica et Biophysica Acta* 1773 (8). NIH Public Access: 1263–84. doi:10.1016/j.bbamcr.2006.10.001.
- McCubrey, James A., Linda S. Steelman, William H. Chappell, Stephen L. Abrams, Ellis W.T. Wong, Fumin Chang, Brian Lehmann, et al. 2007b. "Roles of the Raf/MEK/ERK Pathway in Cell Growth, Malignant Transformation and Drug Resistance." *Biochimica et Biophysica Acta (BBA) - Molecular Cell Research* 1773 (8): 1263–84. doi:10.1016/j.bbamcr.2006.10.001.
- McDaniel, W F, and J C Tucker. 1992. "A Rapid Technique for Visualizing Cerebral Arteries in Rat." *Behavioral and Neural Biology* 58 (3): 242–44. <http://www.ncbi.nlm.nih.gov/pubmed/1280949>.
- Metildi, Cristina A, Sharmeela Kaushal, Chanae R Hardamon, Cynthia S Snyder, Minya Pu, Karen S Messer, Mark A Talamini, Robert M Hoffman, and Michael Bouvet. 2012. "Fluorescence-Guided Surgery Allows for More Complete Resection of Pancreatic Cancer, Resulting in Longer Disease-Free Survival Compared with Standard Surgery in Orthotopic Mouse Models." *Journal of the American College of Surgeons* 215 (1): 126–35; discussion 135–36. doi:10.1016/j.jamcollsurg.2012.02.021.
- Millon, Stacy R, Julie H Ostrander, Siavash Yazdanfar, J Quincy Brown, Janelle E Bender, Anita Rajeha, and Nirmala Ramanujam. "Preferential Accumulation of 5-Aminolevulinic Acid-Induced Protoporphyrin IX in Breast

- Cancer: A Comprehensive Study on Six Breast Cell Lines with Varying Phenotypes." *Journal of Biomedical Optics* 15 (1): 018002.  
doi:10.1117/1.3302811.
- Moiyadi, Aliasgar, Parvez Syed, and Sanjeeva Srivastava. 2014. "Fluorescence-Guided Surgery of Malignant Gliomas Based on 5-Aminolevulinic Acid: Paradigm Shifts but Not a Panacea." *Nature Reviews. Cancer* 14 (2): 146.  
doi:10.1038/nrc3566-c1.
- Mondal, Suman B, Shengkui Gao, Nan Zhu, Rongguang Liang, Viktor Gruev, and Samuel Achilefu. 2014. "Real-Time Fluorescence Image-Guided Oncologic Surgery." *Advances in Cancer Research* 124 (January): 171–211.  
doi:10.1016/B978-0-12-411638-2.00005-7.
- Montagut, Clara, and Jeff Settleman. 2009. "Targeting the RAF-MEK-ERK Pathway in Cancer Therapy." *Cancer Letters* 283 (2): 125–34.  
doi:10.1016/j.canlet.2009.01.022.
- Moon, Dong-Oh, Cheol Park, Moon-Soo Heo, Yeong-Min Park, Yung Hyun Choi, and Gi-Young Kim. 2007. "PD98059 Triggers G1 Arrest and Apoptosis in Human Leukemic U937 Cells through Downregulation of Akt Signal Pathway." *International Immunopharmacology* 7 (1): 36–45.  
doi:10.1016/j.intimp.2006.08.009.
- MOORE, G E, and W T PEYTON. 1948. "The Clinical Use of Fluorescein in Neurosurgery; the Localization of Brain Tumors." *Journal of Neurosurgery* 5 (4): 392–98. doi:10.3171/jns.1948.5.4.0392.
- Morimoto, Kuniyuki, Toshiyuki Ozawa, Kunio Awazu, Nobuhisa Ito, Norihiro Honda, Sohkiichi Matsumoto, and Daisuke Tsuruta. 2014. "Photodynamic Therapy Using Systemic Administration of 5-Aminolevulinic Acid and a 410-Nm Wavelength Light-Emitting Diode for Methicillin-Resistant Staphylococcus Aureus-Infected Ulcers in Mice." *PloS One* 9 (8). Public Library of Science: e105173. doi:10.1371/journal.pone.0105173.

- Nguyen, Quyen T, and Roger Y Tsien. 2013. "Fluorescence-Guided Surgery with Live Molecular Navigation--a New Cutting Edge." *Nature Reviews. Cancer* 13 (9). Nature Publishing Group: 653–62. doi:10.1038/nrc3566.
- Oikonomou, Eftychia, Evangelos Koustas, Maria Goulielmaki, and Alexander Pintzas. 2014. "BRAF vs RAS Oncogenes: Are Mutations of the Same Pathway Equal? Differential Signalling and Therapeutic Implications." *Oncotarget* 5 (23): 11752–77. doi:10.18632/oncotarget.2555.
- Olsson, Ulf, Annika Billberg, Sara Sjövall, Salam Al-Karadaghi, and Mats Hansson. 2002. "In Vivo and in Vitro Studies of Bacillus Subtilis Ferrochelatase Mutants Suggest Substrate Channeling in the Heme Biosynthesis Pathway." *Journal of Bacteriology* 184 (14): 4018–24. <http://www.pubmedcentral.nih.gov/articlerender.fcgi?artid=135158&tool=pmc-entrez&rendertype=abstract>.
- Ortel, B, D Sharlin, D O'Donnell, A K Sinha, E V Maytin, and T Hasan. 2002. "Differentiation Enhances Aminolevulinic Acid-Dependent Photodynamic Treatment of LNCaP Prostate Cancer Cells." *British Journal of Cancer* 87 (11): 1321–27. doi:10.1038/sj.bjc.6600575.
- Papsidero, L D, M Kuriyama, M C Wang, J Horoszewicz, S S Leong, L Valenzuela, G P Murphy, and T M Chu. 1981. "Prostate Antigen: A Marker for Human Prostate Epithelial Cells." *Journal of the National Cancer Institute* 66 (1): 37–42. <http://www.ncbi.nlm.nih.gov/pubmed/6935463>.
- Peng, Q, T Warloe, K Berg, J Moan, M Kongshaug, K E Giercksky, and J M Nesland. 1997. "5-Aminolevulinic Acid-Based Photodynamic Therapy. Clinical Research and Future Challenges." *Cancer* 79 (12): 2282–2308. <http://www.ncbi.nlm.nih.gov/pubmed/9191516>.
- Phelps, R M, B E Johnson, D C Ihde, A F Gazdar, D P Carbone, P R McClintock, R I Linnoila, et al. 1996. "NCI-Navy Medical Oncology Branch Cell Line Data Base." *Journal of Cellular Biochemistry. Supplement* 24 (January): 32–91.



<http://www.ncbi.nlm.nih.gov/pubmed/8806092>.

“Photodynamic Therapy.” 2016. Accessed May 8.

<http://www.cancer.org/treatment/treatmentsandsideeffects/treatmenttypes/photodynamic-therapy>.

Pichlmeier, U., A. Bink, G. Schackert, and W. Stummer. 2008. “Resection and Survival in Glioblastoma Multiforme: An RTOG Recursive Partitioning Analysis of ALA Study Patients.” *Neuro-Oncology* 10 (6): 1025–34. doi:10.1215/15228517-2008-052.

Piot, Benoît, Nathalie Rousset, Peter Lenz, Sabine Eléouet, Jérôme Carré, Véronique Vonarx, Ludovic Bourré, and Thierry Patrice. 2001. “Enhancement of Delta Aminolevulinic Acid-Photodynamic Therapy In Vivo by Decreasing Tumor pH With Glucose and Amiloride.” *The Laryngoscope* 111 (12): 2205–13. doi:10.1097/00005537-200112000-00026.

Pogue, Brian W, Summer Gibbs-Strauss, Pablo A Valdés, Kimberley Samkoe, David W Roberts, and Keith D Paulsen. 2010. “Review of Neurosurgical Fluorescence Imaging Methodologies.” *IEEE Journal of Selected Topics in Quantum Electronics : A Publication of the IEEE Lasers and Electro-Optics Society* 16 (3): 493–505. doi:10.1109/JSTQE.2009.2034541.

Pulaski, B A, V K Clements, M R Pipeling, and S Ostrand-Rosenberg. 2000. “Immunotherapy with Vaccines Combining MHC Class II/CD80+ Tumor Cells with Interleukin-12 Reduces Established Metastatic Disease and Stimulates Immune Effectors and Monokine Induced by Interferon Gamma.” *Cancer Immunology, Immunotherapy : CII* 49 (1): 34–45. <http://www.ncbi.nlm.nih.gov/pubmed/10782864>.

Ragaz, J, S M Jackson, N Le, I H Plenderleith, J J Spinelli, V E Basco, K S Wilson, et al. 1997. “Adjuvant Radiotherapy and Chemotherapy in Node-Positive Premenopausal Women with Breast Cancer.” *The New England Journal of Medicine* 337 (14): 956–62. doi:10.1056/NEJM199710023371402.

- Raguz, S, and E Yagüe. 2008. "Resistance to Chemotherapy: New Treatments and Novel Insights into an Old Problem." *British Journal of Cancer* 99 (3). Cancer Research UK: 387–91. doi:10.1038/sj.bjc.6604510.
- Ramanujam, N. "Fluorescence Spectroscopy of Neoplastic and Non-Neoplastic Tissues." *Neoplasia (New York, N. Y.)* 2 (1-2): 89–117.  
<http://www.pubmedcentral.nih.gov/articlerender.fcgi?artid=1531869&tool=pmcentrez&rendertype=abstract>.
- Roberts, P J, and C J Der. 2007. "Targeting the Raf-MEK-ERK Mitogen-Activated Protein Kinase Cascade for the Treatment of Cancer." *Oncogene* 26 (22): 3291–3310. doi:10.1038/sj.onc.1210422.
- Robey, Robert W, Kenneth Steadman, Orsolya Polgar, and Susan E Bates. 2005. "ABCG2-Mediated Transport of Photosensitizers: Potential Impact on Photodynamic Therapy." *Cancer Biology & Therapy* 4 (2): 187–94.  
<http://www.ncbi.nlm.nih.gov/pubmed/15684613>.
- Sandanaraj, Britto S, Hans-Ulrich Gremlich, Rainer Kneuer, Janet Dawson, and Stefan Wacha. 2010. "Fluorescent Nanoprobes as a Biomarker for Increased Vascular Permeability: Implications in Diagnosis and Treatment of Cancer and Inflammation." *Bioconjugate Chemistry* 21 (1): 93–101.  
doi:10.1021/bc900311h.
- Sevick-Muraca, Eva M, and John C Rasmussen. "Molecular Imaging with Optics: Primer and Case for near-Infrared Fluorescence Techniques in Personalized Medicine." *Journal of Biomedical Optics* 13 (4): 041303.  
doi:10.1117/1.2953185.
- Shao, Peng, David W Chapman, Ronald B Moore, and Roger J Zemp. 2015. "Monitoring Photodynamic Therapy with Photoacoustic Microscopy." *Journal of Biomedical Optics* 20 (10): 106012. doi:10.1117/1.JBO.20.10.106012.
- Siegel, Rebecca L., Kimberly D. Miller, and Ahmedin Jemal. 2015. "Cancer

Statistics, 2016.” *CA: A Cancer Journal for Clinicians* 66 (1): n/a – n/a.  
doi:10.3322/caac.21332.

Silva, Scott, Anil Sethi, Vikram Prabhu, Douglas Anderson, and Edward Melian. 2015. “MNGO-19RETROSPECTIVE REVIEW OF OVERALL SURVIVAL IN MENINGIOMA PATIENTS TREATED WITH RADIOTHERAPY OR COMBINED RADIOTHERAPY AND SURGERY.” *Neuro-Oncology* 17 (suppl 5). Oxford University Press: v134.1–v134. doi:10.1093/neuonc/nov220.18.

Singh, Yashveer, Matthew Palombo, and Patrick J Sinko. 2008. “Recent Trends in Targeted Anticancer Prodrug and Conjugate Design.” *Current Medicinal Chemistry* 15 (18): 1802–26.  
<http://www.pubmedcentral.nih.gov/articlerender.fcgi?artid=2802226&tool=pmcentrez&rendertype=abstract>.

Sivabalan, Shanmugam, C Ponranjini Vedeswari, Sadaksharam Jayachandran, Dornadula Koteeswaran, Chidambaranathan Pravda, Prakasa Rao Aruna, and Singaravelu Ganesan. “In Vivo Native Fluorescence Spectroscopy and Nicotinamide Adenine Dinucleotide/flavin Adenine Dinucleotide Reduction and Oxidation States of Oral Submucous Fibrosis for Chemopreventive Drug Monitoring.” *Journal of Biomedical Optics* 15 (1): 017010.  
doi:10.1117/1.3324771.

Sramkoski, R M, T G Pretlow, J M Giaconia, T P Pretlow, S Schwartz, M S Sy, S R Marengo, J S Rhim, D Zhang, and J W Jacobberger. “A New Human Prostate Carcinoma Cell Line, 22Rv1.” *In Vitro Cellular & Developmental Biology. Animal* 35 (7): 403–9. doi:10.1007/s11626-999-0115-4.

Stummer, W, A Novotny, H Stepp, C Goetz, K Bise, and H J Reulen. 2000. “Fluorescence-Guided Resection of Glioblastoma Multiforme by Using 5-Aminolevulinic Acid-Induced Porphyrins: A Prospective Study in 52 Consecutive Patients.” *Journal of Neurosurgery* 93 (6): 1003–13.  
doi:10.3171/jns.2000.93.6.1003.

- Stummer, W, H Stepp, G Möller, A Ehrhardt, M Leonhard, and H J Reulen. 1998. "Technical Principles for Protoporphyrin-IX-Fluorescence Guided Microsurgical Resection of Malignant Glioma Tissue." *Acta Neurochirurgica* 140 (10): 995–1000. <http://www.ncbi.nlm.nih.gov/pubmed/9856241>.
- Sugarman, B J, B B Aggarwal, P E Hass, I S Figari, M A Palladino, and H M Shepard. 1985. "Recombinant Human Tumor Necrosis Factor-Alpha: Effects on Proliferation of Normal and Transformed Cells in Vitro." *Science (New York, N.Y.)* 230 (4728): 943–45. <http://www.ncbi.nlm.nih.gov/pubmed/3933111>.
- Sun, Xiao-xiao, and Qiang Yu. 2015. "Intra-Tumor Heterogeneity of Cancer Cells and Its Implications for Cancer Treatment." *Acta Pharmacologica Sinica* 36 (10): 1219–27. doi:10.1038/aps.2015.92.
- To, Kenneth K W, and Brian Tomlinson. 2013. "Targeting the ABCG2-Overexpressing Multidrug Resistant (MDR) Cancer Cells by PPAR $\gamma$  Agonists." *British Journal of Pharmacology* 170 (5): 1137–51. doi:10.1111/bph.12367.
- Vahrmeijer, Alexander L., Merlijn Hutteman, Joost R. van der Vorst, Cornelis J. H. van de Velde, and John V. Frangioni. 2013. "Image-Guided Cancer Surgery Using near-Infrared Fluorescence." *Nature Reviews Clinical Oncology* 10 (9). Nature Publishing Group: 507–18. doi:10.1038/nrclinonc.2013.123.
- Valdés, Pablo A, Anthony Kim, Marco Brantsch, Carolyn Niu, Ziev B Moses, Tor D Tosteson, Brian C Wilson, Keith D Paulsen, David W Roberts, and Brent T Harris. 2011. "δ-Aminolevulinic Acid-Induced Protoporphyrin IX Concentration Correlates with Histopathologic Markers of Malignancy in Human Gliomas: The Need for Quantitative Fluorescence-Guided Resection to Identify Regions of Increasing Malignancy." *Neuro-Oncology* 13 (8): 846–56. doi:10.1093/neuonc/nor086.

- Vanneman, Matthew, and Glenn Dranoff. 2012. "Combining Immunotherapy and Targeted Therapies in Cancer Treatment." *Nature Reviews. Cancer* 12 (4): 237–51. doi:10.1038/nrc3237.
- Wan, Kayiu, Bernd Ebert, Jan Voigt, Qing Wang, Yiyang Dai, Rainer Haag, and Wolfgang Kimmner. 2012. "In Vivo Tumor Imaging Using a Novel RNAi-Based Detection Mechanism." *Nanomedicine : Nanotechnology, Biology, and Medicine* 8 (4): 393–98. doi:10.1016/j.nano.2012.02.004.
- Wang, Chunlei, Xiaofeng Chen, Jianing Wu, Huailei Liu, Zhiyong Ji, Huaizhang Shi, Cheng Gao, et al. 2013. "Low-Dose Arsenic Trioxide Enhances 5-Aminolevulinic Acid-Induced PpIX Accumulation and Efficacy of Photodynamic Therapy in Human Glioma." *Journal of Photochemistry and Photobiology. B, Biology* 127 (October): 61–67. doi:10.1016/j.jphotobiol.2013.06.001.
- Wezgowiec, Joanna, Maria B Derylo, Justin Teissie, Julie Orio, Marie-Pierre Rols, Julita Kulbacka, Jolanta Saczko, and Malgorzata Kotulska. 2013. "Electric Field-Assisted Delivery of Photofrin to Human Breast Carcinoma Cells." *The Journal of Membrane Biology* 246 (10): 725–35. doi:10.1007/s00232-013-9533-z.
- Xie, Jin, Bin Jin, Da-Wei Li, Bin Shen, Ning Cong, Tian-Zhen Zhang, and Pin Dong. 2014. "ABCG2 Regulated by MAPK Pathways Is Associated with Cancer Progression in Laryngeal Squamous Cell Carcinoma." *American Journal of Cancer Research* 4 (6): 698–709. <http://www.pubmedcentral.nih.gov/articlerender.fcgi?artid=4266705&tool=pmcentrez&rendertype=abstract>.
- Yamamoto, Masanao, Hirofumi Fujita, Naoki Katase, Keiji Inoue, Hitoshi Nagatsuka, Kozo Utsumi, Junzo Sasaki, and Hideyo Ohuchi. 2013. "Improvement of the Efficacy of 5-Aminolevulinic Acid-Mediated Photodynamic Treatment in Human Oral Squamous Cell Carcinoma HSC-4."

*Acta Medica Okayama* 67 (3): 153–64.

<http://www.ncbi.nlm.nih.gov/pubmed/23804138>.

Zhang, Guang, Zhongxia Wang, Weihuan Luo, Hongbo Jiao, Junhua Wu, and Chunping Jiang. 2013. “Expression of Potential Cancer Stem Cell Marker ABCG2 Is Associated with Malignant Behaviors of Hepatocellular Carcinoma.” *Gastroenterology Research and Practice* 2013 (January): 782581. doi:10.1155/2013/782581.

Zhang, Wei, and Hui Tu Liu. 2002. “MAPK Signal Pathways in the Regulation of Cell Proliferation in Mammalian Cells.” *Cell Research* 12 (1): 9–18. doi:10.1038/sj.cr.7290105.

Zhao, Shiguang, Jianing Wu, Chunlei Wang, Huailei Liu, Xingli Dong, Chen Shi, Changbin Shi, et al. 2013. “Intraoperative Fluorescence-Guided Resection of High-Grade Malignant Gliomas Using 5-Aminolevulinic Acid-Induced Porphyrins: A Systematic Review and Meta-Analysis of Prospective Studies.” *PloS One* 8 (5): e63682. doi:10.1371/journal.pone.0063682.

Zhao, Yujie, and Alex A Adjei. 2014. “The Clinical Development of MEK Inhibitors.” *Nature Reviews. Clinical Oncology* 11 (7): 385–400. doi:10.1038/nrclinonc.2014.83.

Zhou, Sheng, Yang Zong, Paul A Ney, Geeta Nair, Clinton F Stewart, and Brian P Sorrentino. 2005. “Increased Expression of the Abcg2 Transporter during Erythroid Maturation Plays a Role in Decreasing Cellular Protoporphyrin IX Levels.” *Blood* 105 (6): 2571–76. doi:10.1182/blood-2004-04-1566.